

# Dark matter models with (pseudo)scalar mediators

Pyungwon Ko (KIAS)

HPNP2017, Toyama, Japan  
Mar. 1-5 (2017)

# Contents

- Higgs portal singlet fermion/vector DM models :
  - EFT vs. renormalizable, gauge invariant, unitary models
  - GC gamma ray excess, Collider Signatures
- Pseudoscalar portal DM models

Related talks by M. Kakizaki,  
Jinsu Kim, Toshinori Matsui on  
**Gravitational waves, Higgs inflation**

# Higgs portal DM models

$$\mathcal{L}_{\text{scalar}} = \frac{1}{2} \partial_\mu S \partial^\mu S - \frac{1}{2} m_S^2 S^2 - \frac{\lambda_{HS}}{2} H^\dagger H S^2 - \frac{\lambda_S}{4} S^4$$

$$\mathcal{L}_{\text{fermion}} = \overline{\psi} [i\gamma \cdot \partial - m_\psi] \psi - \frac{\lambda_{H\psi}}{\Lambda} H^\dagger H \overline{\psi} \psi$$

$$\mathcal{L}_{\text{vector}} = -\frac{1}{4} V_{\mu\nu} V^{\mu\nu} + \frac{1}{2} m_V^2 V_\mu V^\mu + \frac{1}{4} \lambda_V (V_\mu V^\mu)^2 + \frac{1}{2} \lambda_{HV} H^\dagger H V_\mu V^\mu.$$

All invariant  
under ad hoc  
Z2 symmetry

arXiv:1112.3299, ... 1402.6287, etc.

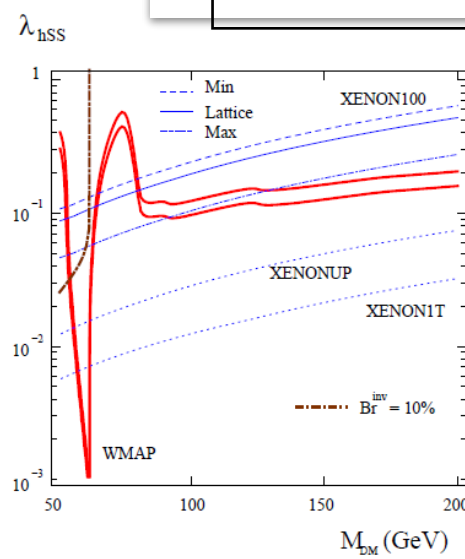


FIG. 1. Scalar Higgs-portal parameter space allowed by WMAP (between the solid red curves), XENON100 and  $\text{Br}^{\text{inv}} = 10\%$  for  $m_h = 125$  GeV. Shown also are the prospects for XENON upgrades.

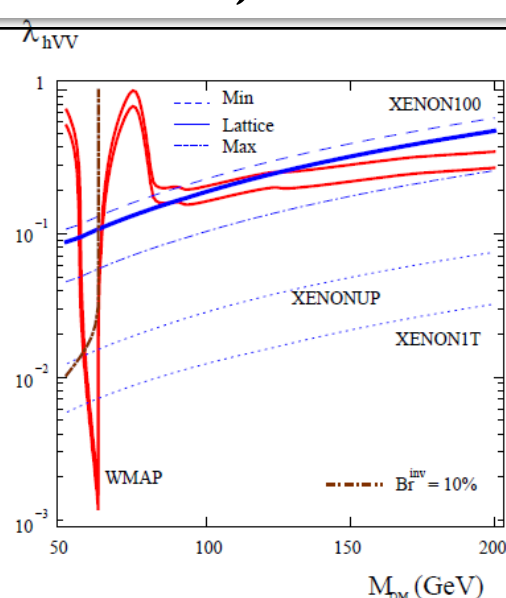


FIG. 2. Same as Fig. 1 for vector DM particles.

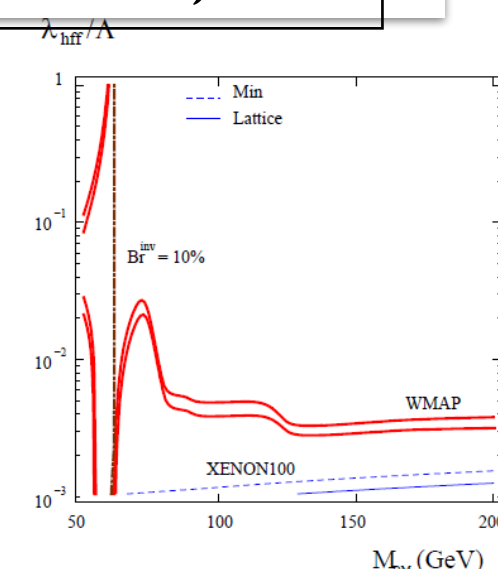


FIG. 3. Same as in Fig. 1 for fermion DM;  $\lambda_{hff}/\Lambda$  is in  $\text{GeV}^{-1}$ .

# Higgs portal DM models

$$\mathcal{L}_{\text{scalar}} = \frac{1}{2}\partial_\mu S \partial^\mu S - \frac{1}{2}m_S^2 S^2 - \frac{\lambda_{HS}}{2} H^\dagger H S^2 - \frac{\lambda_S}{4} S^4$$

$$\mathcal{L}_{\text{fermion}} = \bar{\psi} [i\gamma \cdot \partial - m_\psi] \psi - \frac{\lambda_{H\psi}}{\Lambda} H^\dagger H \bar{\psi} \psi$$

$$\mathcal{L}_{\text{vector}} = -\frac{1}{4}V_{\mu\nu}V^{\mu\nu} + \frac{1}{2}m_V^2 V_\mu V^\mu + \frac{1}{4}\lambda_V(V_\mu V^\mu)^2 + \frac{1}{2}\lambda_{HV}H^\dagger H V_\mu V^\mu.$$

All invariant  
under ad hoc  
 $\mathbb{Z}_2$  symmetry

- Scalar CDM : looks OK, renorm.. BUT .....
- Fermion CDM : nonrenormalizable
- Vector CDM : looks OK, but it has a number of problems (in fact, it is not renormalizable)

# Usual story within EFT

- Strong bounds from direct detection exp's put stringent bounds on the Higgs coupling to the dark matters
- So, the invisible Higgs decay is suppressed
- There is only one SM Higgs boson with the signal strengths equal to ONE if the invisible Higgs decay is ignored
- All these conclusions are not reproduced in the full theories (renormalizable) however

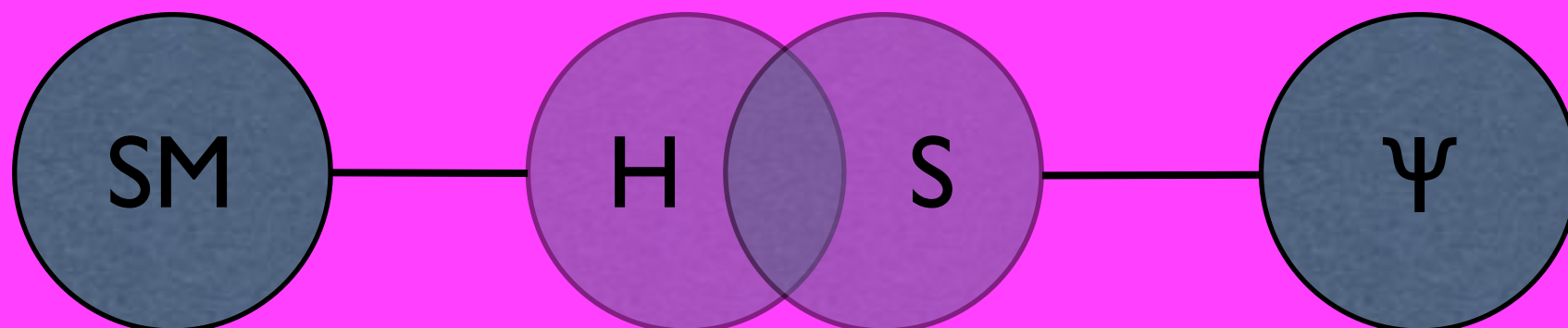
# Singlet fermion CDM

Baek, Ko, Park, arXiv:1112.1847

$$\begin{aligned}\mathcal{L} = \mathcal{L}_{\text{SM}} &+ \mu_{HS} S H^\dagger H - \frac{\lambda_{HS}}{2} S^2 H^\dagger H \\ &+ \frac{1}{2} (\partial_\mu S \partial^\mu S - m_S^2 S^2) - \mu_S^3 S - \frac{\mu'_S}{3} S^3 - \frac{\lambda_S}{4} S^4 \\ &+ \bar{\psi} (i \not{\partial} - m_{\psi_0}) \psi - \lambda S \bar{\psi} \psi\end{aligned}$$

mixing

invisible decay



Production and decay rates are suppressed relative to SM.

This simple model has not been studied properly !!

# Ratiocination

- Mixing and Eigenstates of Higgs-like bosons

$$\begin{aligned}\mu_H^2 &= \lambda_H v_H^2 + \mu_{HS} v_S + \frac{1}{2} \lambda_{HS} v_S^2, \\ m_S^2 &= -\frac{\mu_S^3}{v_S} - \mu'_S v_S - \lambda_S v_S^2 - \frac{\mu_{HS} v_H^2}{2v_S} - \frac{1}{2} \lambda_{HS} v_H^2,\end{aligned}$$

at vacuum

$$M_{\text{Higgs}}^2 \equiv \begin{pmatrix} m_{hh}^2 & m_{hs}^2 \\ m_{hs}^2 & m_{ss}^2 \end{pmatrix} \equiv \begin{pmatrix} \cos \alpha & \sin \alpha \\ -\sin \alpha & \cos \alpha \end{pmatrix} \begin{pmatrix} m_1^2 & 0 \\ 0 & m_2^2 \end{pmatrix} \begin{pmatrix} \cos \alpha & -\sin \alpha \\ \sin \alpha & \cos \alpha \end{pmatrix}$$

$$H_1 = h \cos \alpha - s \sin \alpha,$$

$$H_2 = h \sin \alpha + s \cos \alpha.$$



Mixing of Higgs and singlet

# Ratiocination

- Signal strength (reduction factor)

$$r_i = \frac{\sigma_i \text{ Br}(H_i \rightarrow \text{SM})}{\sigma_h \text{ Br}(h \rightarrow \text{SM})}$$
$$r_1 = \frac{\cos^4 \alpha \Gamma_{H_1}^{\text{SM}}}{\cos^2 \alpha \Gamma_{H_1}^{\text{SM}} + \sin^2 \alpha \Gamma_{H_1}^{\text{hid}}}$$
$$r_2 = \frac{\sin^4 \alpha \Gamma_{H_2}^{\text{SM}}}{\sin^2 \alpha \Gamma_{H_2}^{\text{SM}} + \cos^2 \alpha \Gamma_{H_2}^{\text{hid}} + \Gamma_{H_2 \rightarrow H_1 H_1}}$$

$$0 < \alpha < \pi/2 \Rightarrow r_1(r_2) < 1$$

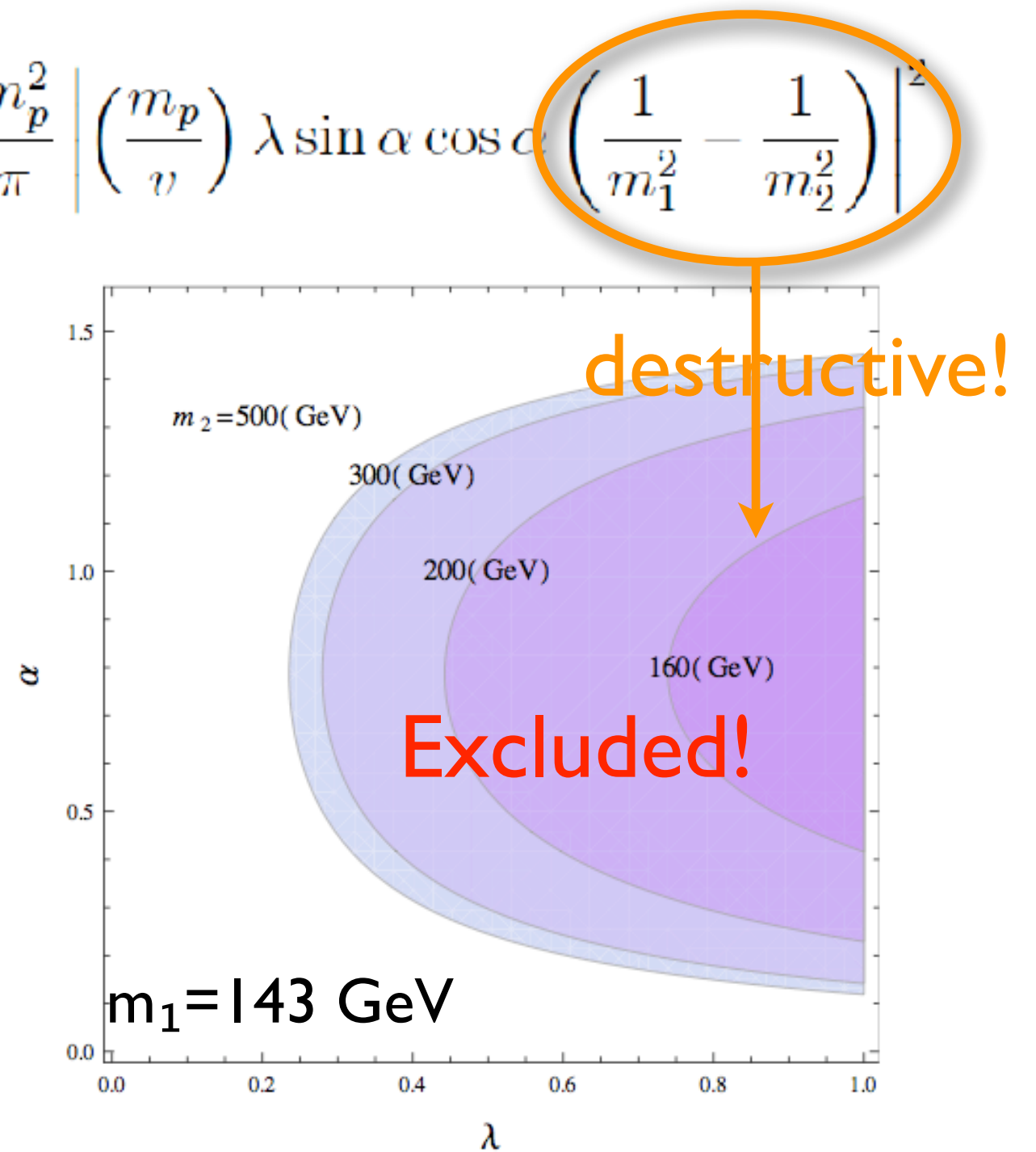
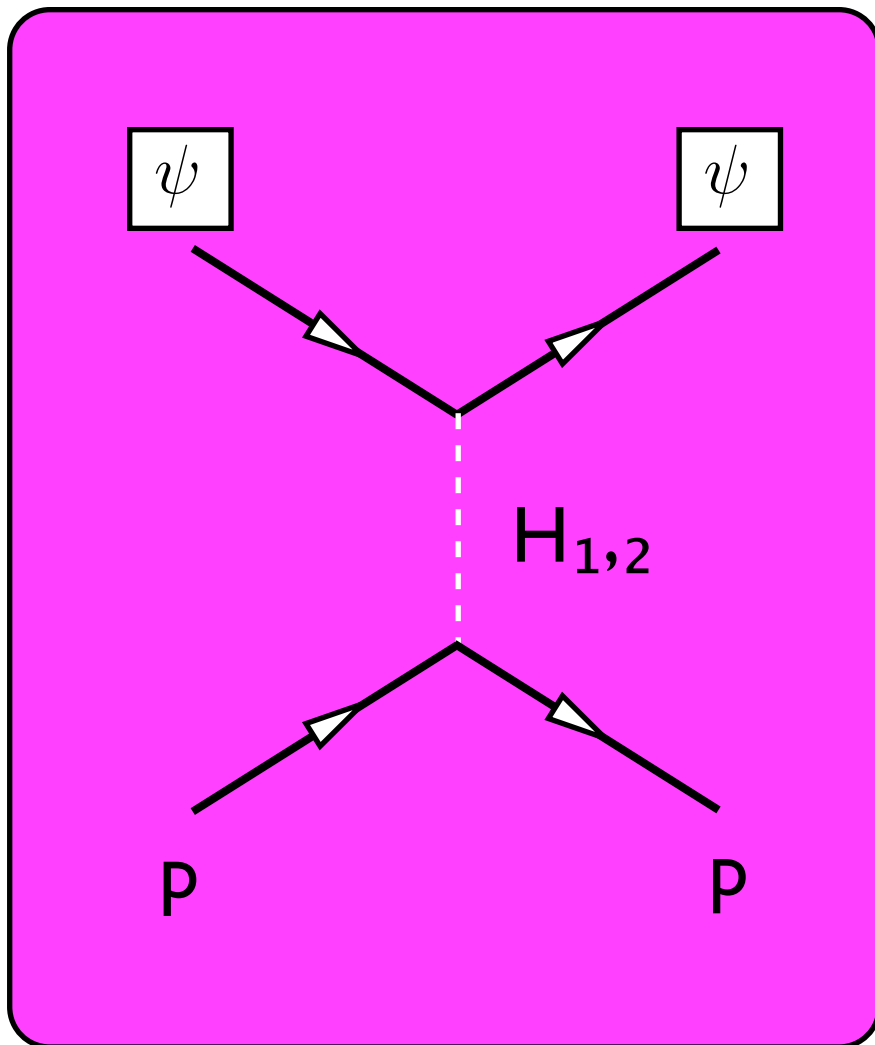
Invisible decay mode is not necessary!

If  $r_i > 1$  for any single channel,  
this model will be excluded !!

# Constraints

- Dark matter to nucleon cross section (constraint)

$$\sigma_p \approx \frac{1}{\pi} \mu^2 \lambda_p^2 \simeq 2.7 \times 10^{-2} \frac{m_p^2}{\pi} \left| \left( \frac{m_p}{v} \right) \lambda \sin \alpha \cos \alpha \left( \frac{1}{m_1^2} - \frac{1}{m_2^2} \right) \right|^2$$



- We don't use the effective lagrangian approach (nonrenormalizable interactions), since we don't know the mass scale related with the CDM

$$\mathcal{L}_{\text{eff}} = \bar{\psi} \left( m_0 + \frac{H^\dagger H}{\Lambda} \right) \psi. \quad \text{or} \quad \lambda h \bar{\psi} \psi$$

Breaks SM gauge sym

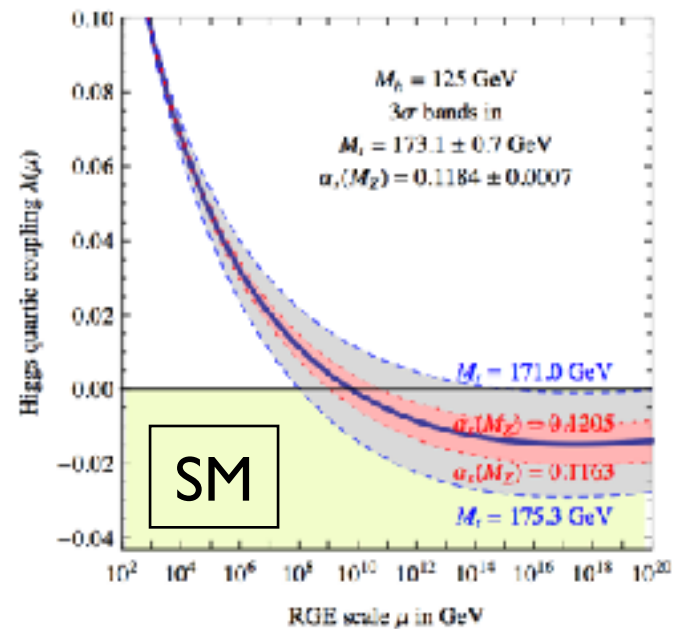
- Only one Higgs boson (alpha = 0)
- We cannot see the cancellation between two Higgs scalars in the direct detection cross section, if we used the above effective lagrangian
- The upper bound on DD cross section gives less stringent bound on the possible invisible Higgs decay

# Low energy pheno.

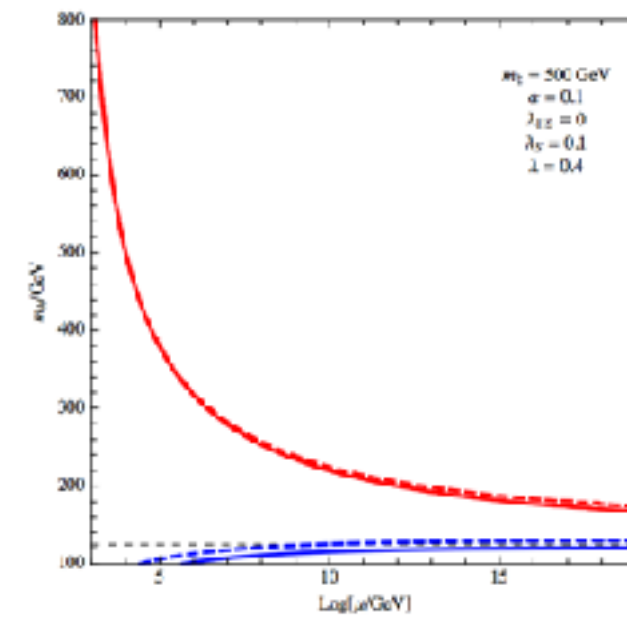
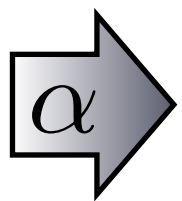
- Universal suppression of collider SM signals  
[See 1112.1847, Seungwon Baek, P. Ko & WIP]
- If “ $m_h > 2 m_\phi$ ”, non-SM Higgs decay!
- Tree-level shift of  $\lambda_{H,\text{SM}}$  (& loop correction)

$$\lambda_{\Phi H} \Rightarrow \lambda_H = \left[ 1 + \left( \frac{m_\phi^2}{m_h^2} - 1 \right) \sin^2 \alpha \right] \lambda_H^{\text{SM}}$$

→ If “ $m_\phi > m_h$ ”, vacuum instability can be cured.

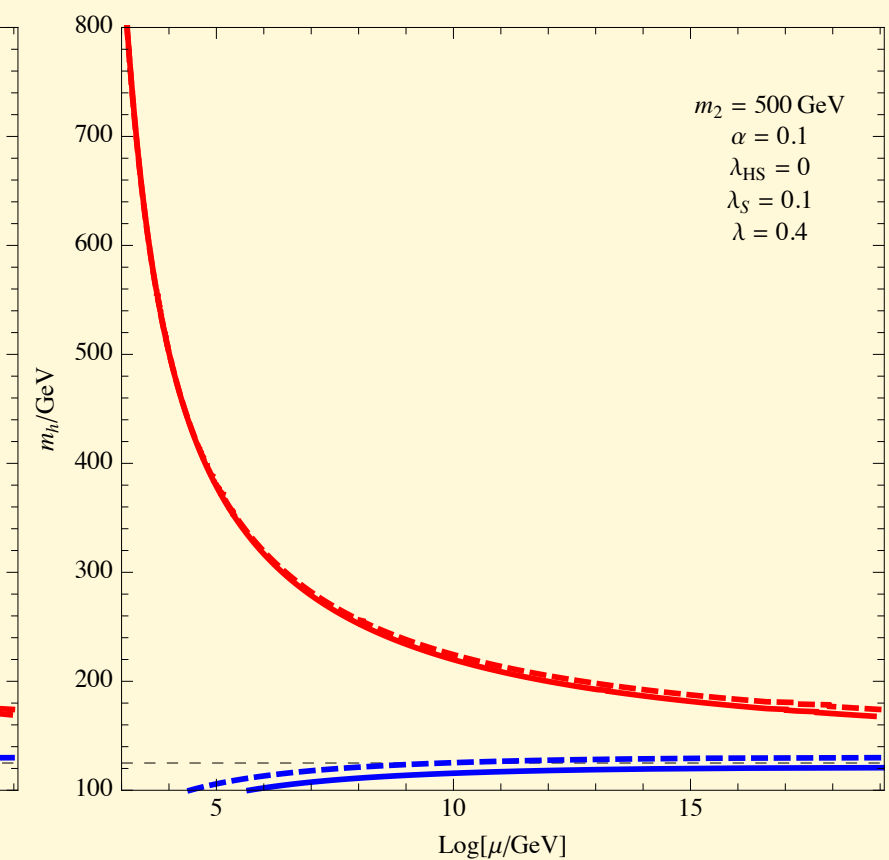
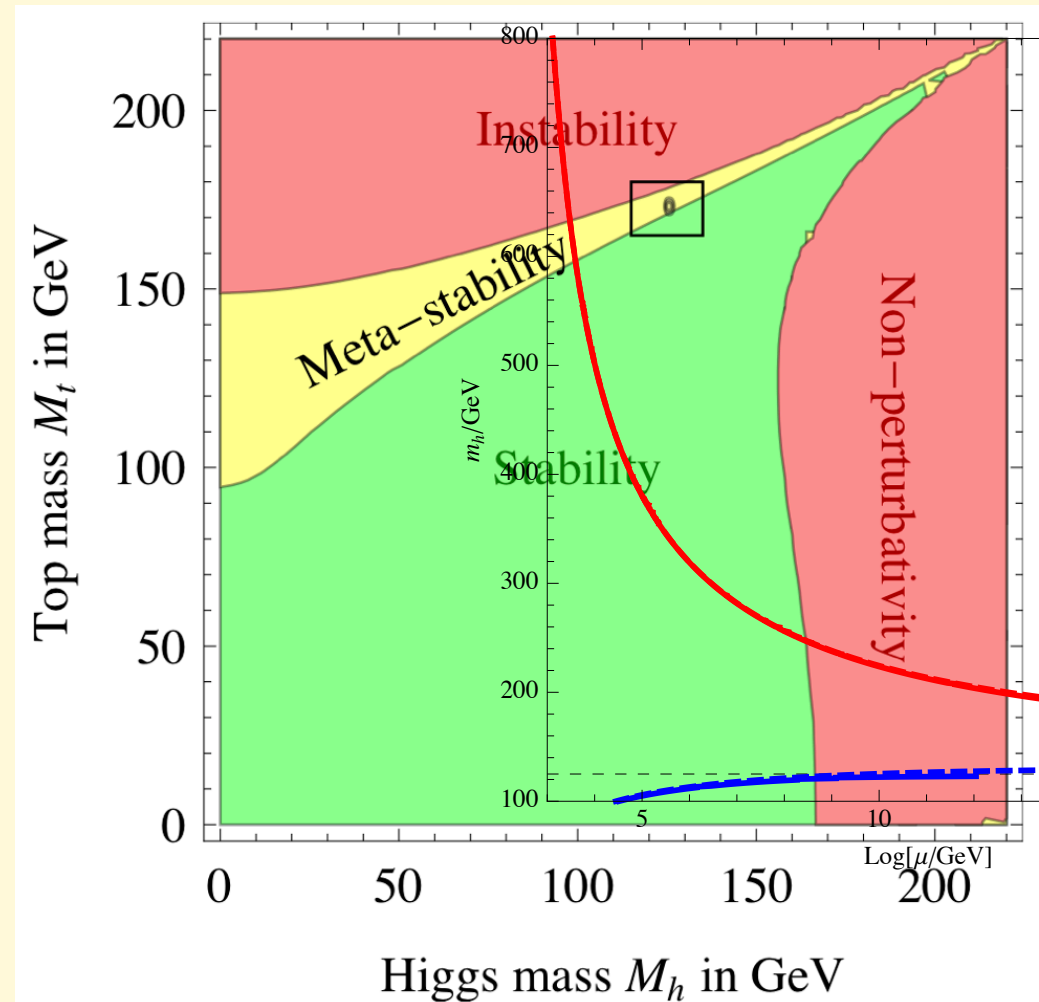


[G. Degrassi et al., 1205.6497]



[S. Baek, P. Ko, WIP & E. Senaha, JHEP(2012)]

# Vacuum Stability Improved by the singlet scalar $S$



A. Strumia, Moriond EW 2013

Baek, Ko, Park, Senaha (2012)

# Similar for Higgs portal Vector DM

$$\mathcal{L} = -m_V^2 V_\mu V^\mu - \frac{\lambda_{VH}}{4} H^\dagger H V_\mu V^\mu - \frac{\lambda_V}{4} (V_\mu V^\mu)^2$$

- Although this model looks renormalizable, it is not really renormalizable, since there is no agency for vector boson mass generation
- Need to a new Higgs that gives mass to VDM
- A complete model should be something like this:

$$\begin{aligned}\mathcal{L}_{VDM} = & -\frac{1}{4}X_{\mu\nu}X^{\mu\nu} + (D_\mu\Phi)^\dagger(D^\mu\Phi) - \frac{\lambda_\Phi}{4}\left(\Phi^\dagger\Phi - \frac{v_\Phi^2}{2}\right)^2 \\ & -\lambda_{H\Phi}\left(H^\dagger H - \frac{v_H^2}{2}\right)\left(\Phi^\dagger\Phi - \frac{v_\Phi^2}{2}\right),\end{aligned}$$

$$\langle 0|\phi_X|0\rangle = v_X + h_X(x)$$

$X_\mu \equiv V_\mu$  here

- There appear a new singlet scalar  $h_X$  from  $\phi_X$ , which mixes with the SM Higgs boson through Higgs portal
- The effects must be similar to the singlet scalar in the fermion CDM model, and generically true in the DM with dark gauge sym
- Important to consider a minimal renormalizable and unitary model to discuss physics correctly [Baek, Ko, Park and Senaha, arXiv: 1212.2131 (JHEP)]
- Can accommodate GeV scale gamma ray excess from GC

# New scalar improves EW vacuum stability

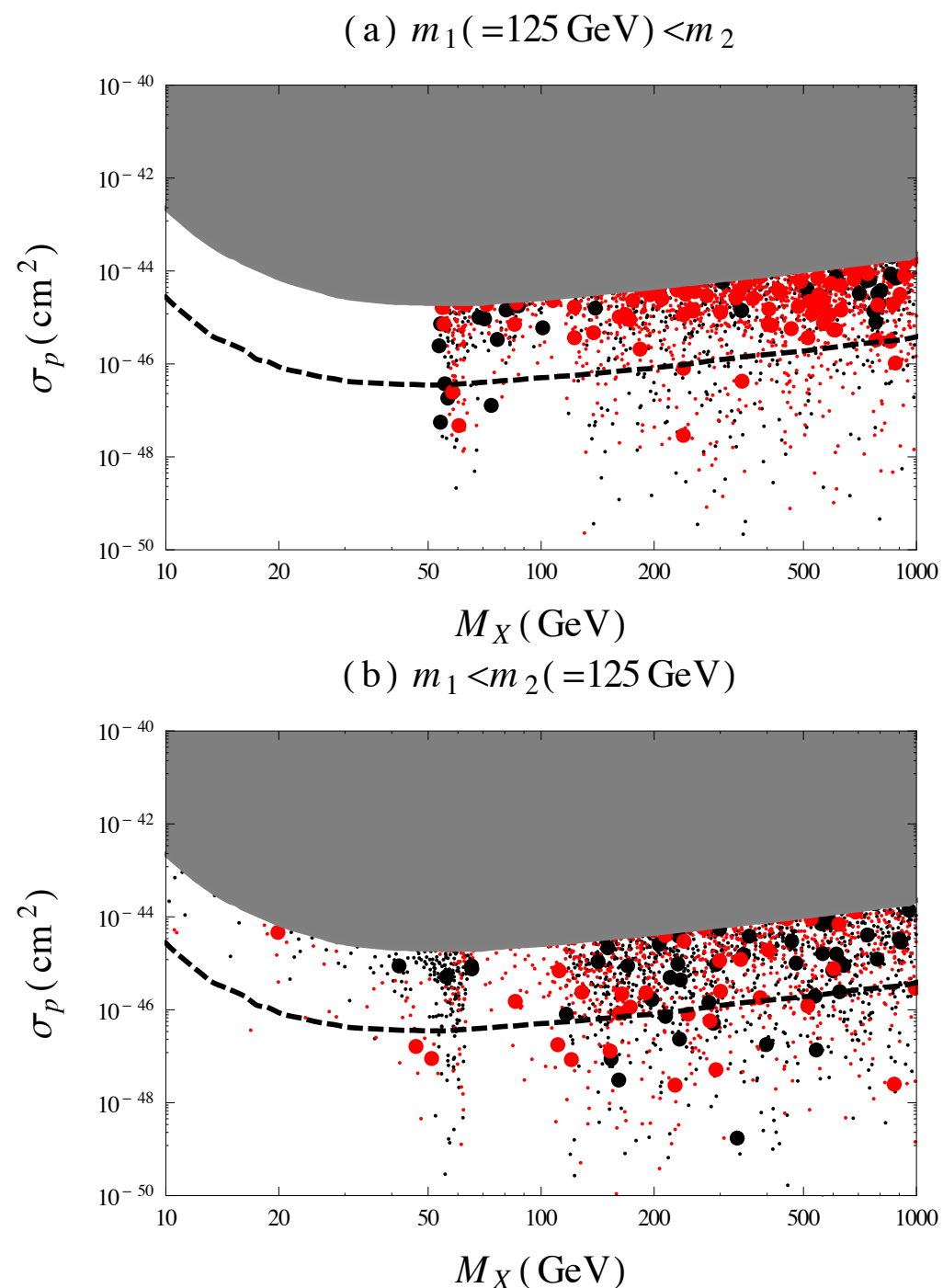


**Figure 6.** The scattered plot of  $\sigma_p$  as a function of  $M_X$ . The big (small) points (do not) satisfy the WMAP relic density constraint within  $3\sigma$ , while the red-(black-)colored points gives  $r_1 > 0.7$  ( $r_1 < 0.7$ ). The grey region is excluded by the XENON100 experiment. The dashed line denotes the sensitivity of the next XENON experiment, XENON1T.

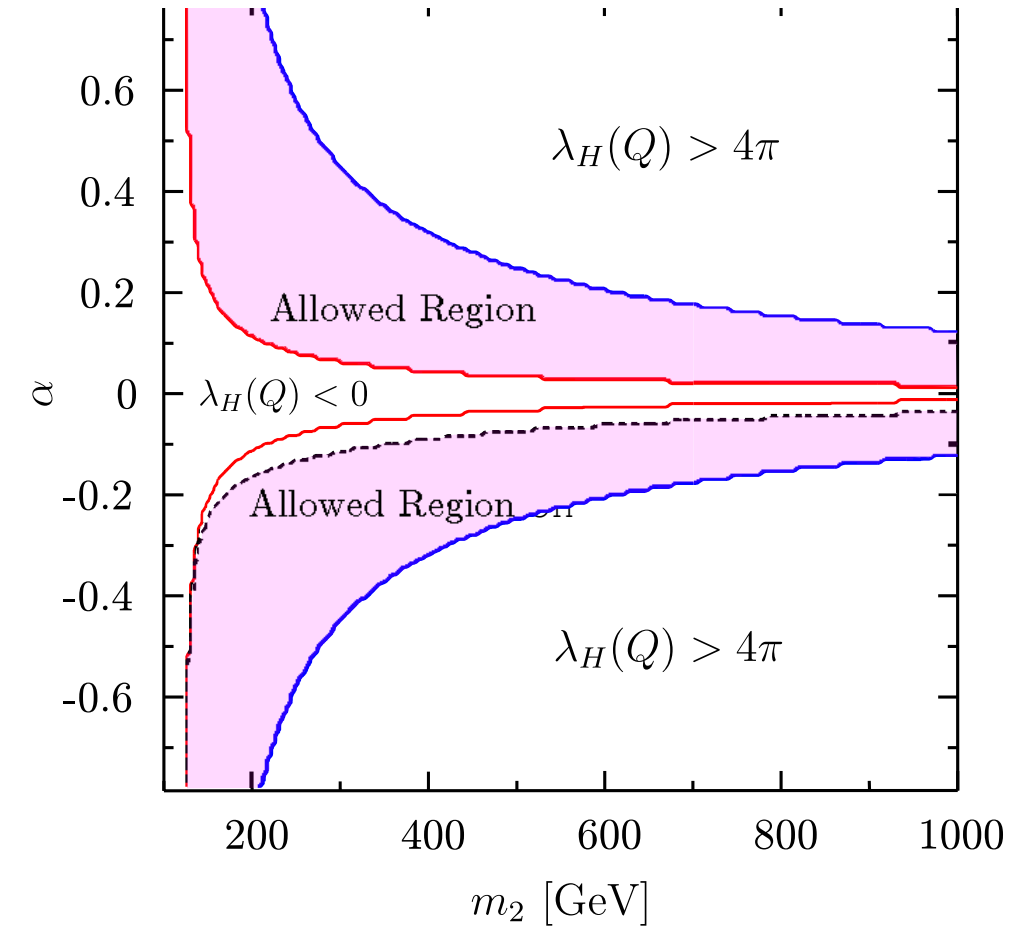


**Figure 8.** The vacuum stability and perturbativity constraints in the  $\alpha$ - $m_2$  plane. We take  $m_1 = 125 \text{ GeV}$ ,  $g_X = 0.05$ ,  $M_X = m_2/2$  and  $v_\Phi = M_X/(g_X Q_\Phi)$ .

# Higgs portal DM as examples

$$\mathcal{L}_{\text{scalar}} = \frac{1}{2}\partial_\mu S \partial^\mu S - \frac{1}{2}m_S^2 S^2 - \frac{\lambda_{HS}}{2}H^\dagger H S^2 - \frac{\lambda_S}{4}S^4$$

$$\mathcal{L}_{\text{fermion}} = \overline{\psi} [i\gamma \cdot \partial - m_\psi] \psi - \frac{\lambda_{H\psi}}{\Lambda} H^\dagger H \overline{\psi} \psi$$

$$\mathcal{L}_{\text{vector}} = -\frac{1}{4}V_{\mu\nu}V^{\mu\nu} + \frac{1}{2}m_V^2 V_\mu V^\mu + \frac{1}{4}\lambda_V(V_\mu V^\mu)^2 + \frac{1}{2}\lambda_{HV}H^\dagger H V_\mu V^\mu.$$

All invariant  
under ad hoc  
Z2 symmetry

arXiv:1112.3299, ... 1402.6287, etc.

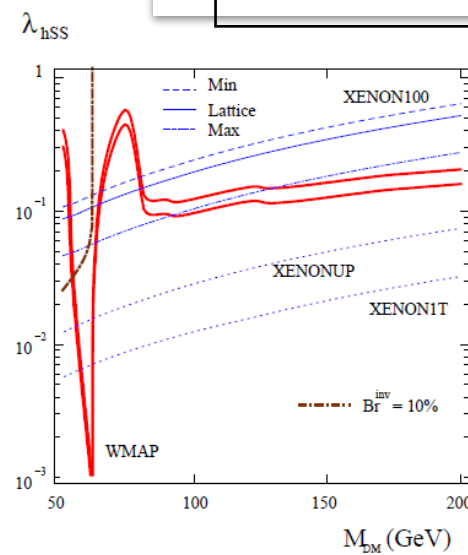


FIG. 1. Scalar Higgs-portal parameter space allowed by WMAP (between the solid red curves), XENON100 and  $\text{Br}^{\text{inv}} = 10\%$  for  $m_h = 125$  GeV. Shown also are the prospects for XENON upgrades.

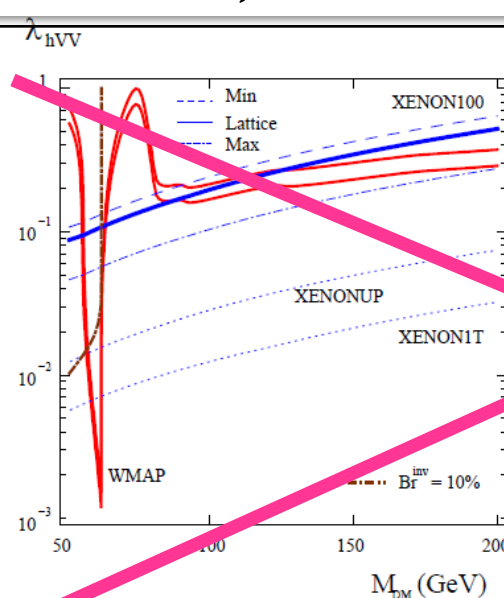


FIG. 2. Same as Fig. 1 for vector DM particles.

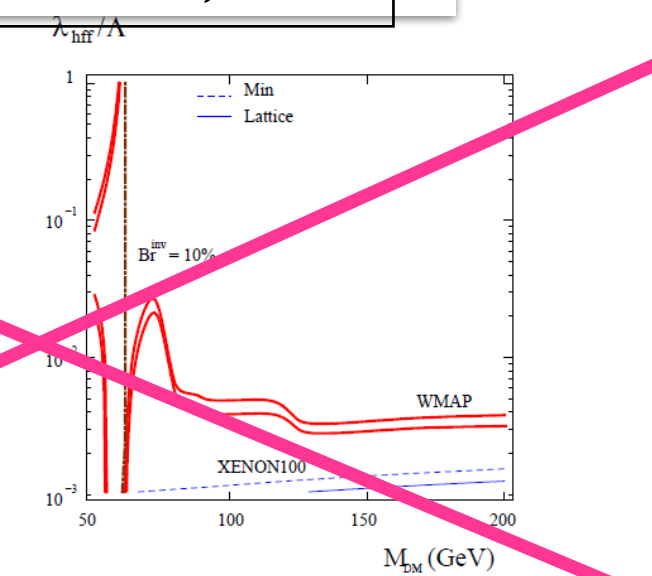


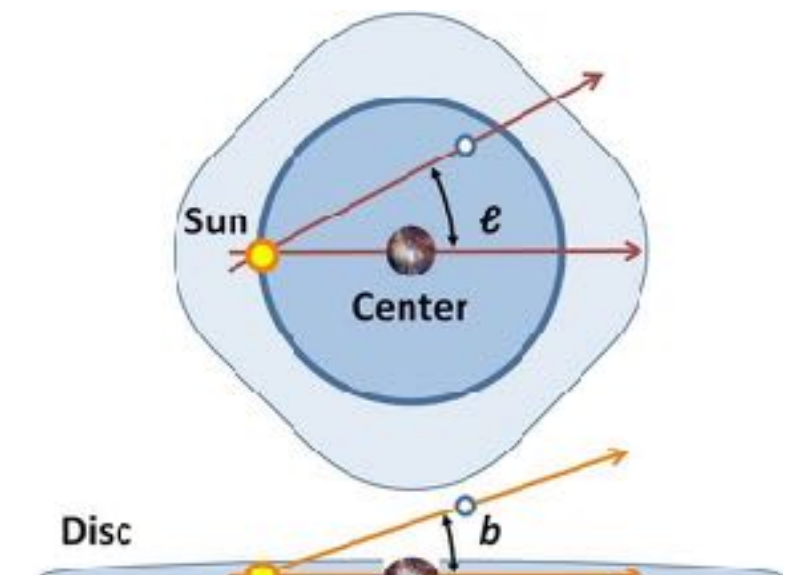
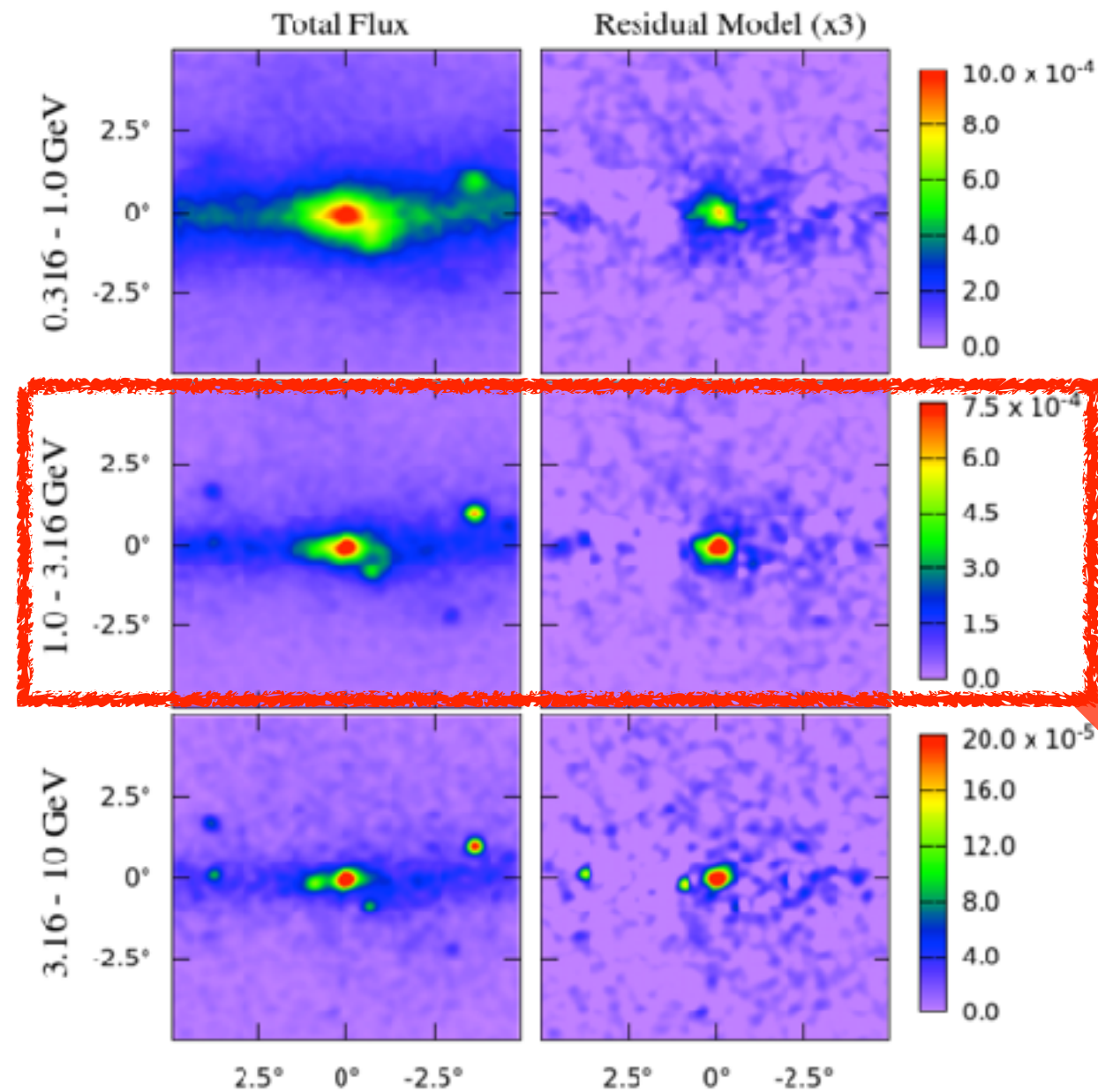
FIG. 3. Same as in Fig. 1 for fermion DM;  $\lambda_{hff}/\Lambda$  is in  $\text{GeV}^{-1}$ .

**Is this any useful in  
phenomenology ?**

**YES !**

# Fermi-LAT $\gamma$ -ray excess

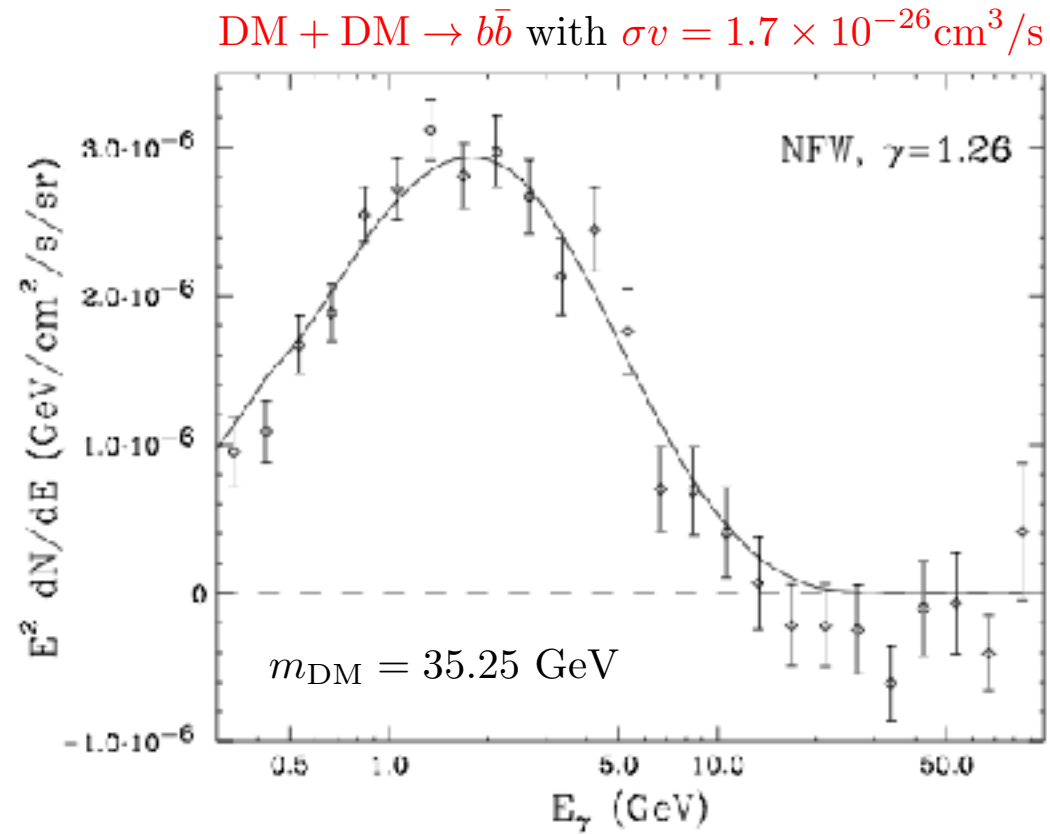
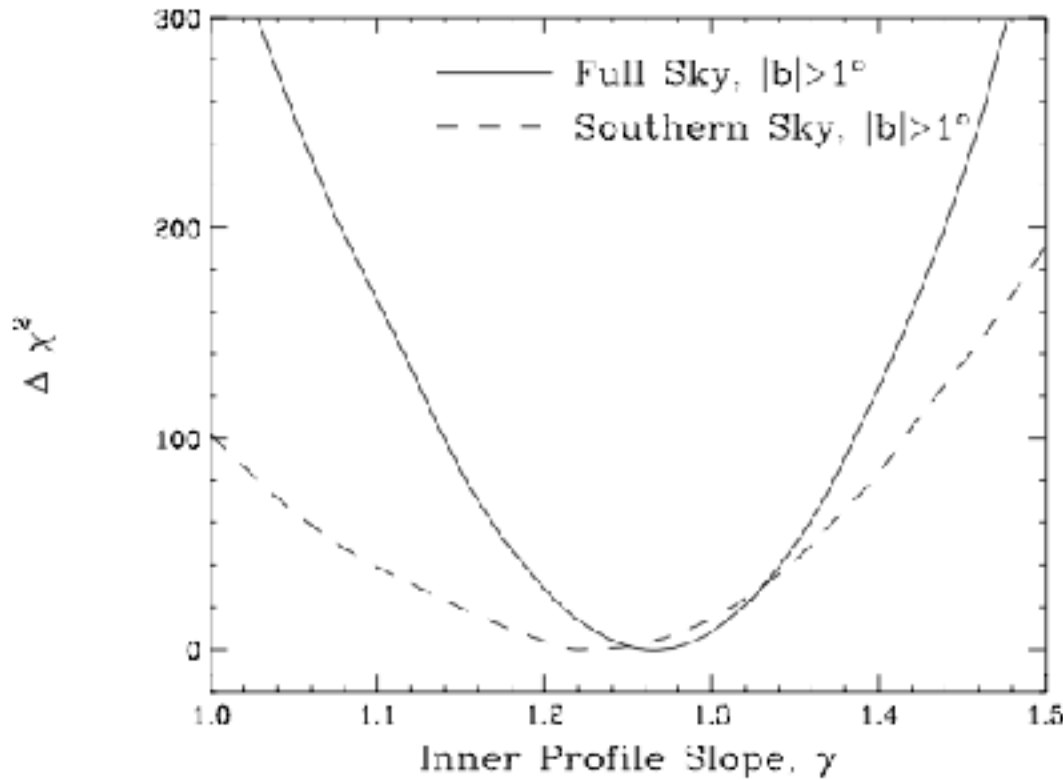
- Gamma-ray excess in the direction of GC



GC :  $b \sim l \lesssim 0.1^\circ$

extended  
GeV scale excess!

## ● A DM interpretation



\* See "1402.6703, T. Daylan et.al." for other possible channels

## ● Millisecond Pulsars (astrophysical alternative)

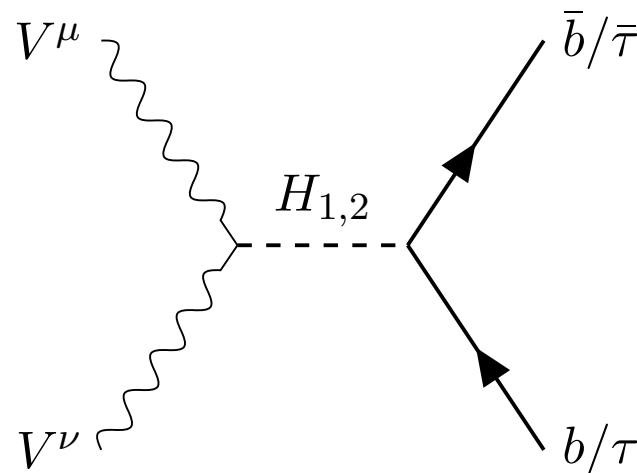
It may or may not be the main source, depending on

- luminosity func.
- bulge population
- distribution of bulge population

\* See "1404.2318, Q.Yuan & B. Zhang" and "1407.5625, I. Cholis, D. Hooper & T. Linden"

# GC gamma ray in VDM

[I404.5257, P.Ko,WIP & Y.Tang] JCAP (2014)  
(Also Celine Boehm et al. I404.4977, PRD)



**H2 : 125 GeV Higgs**  
**H1 : absent in EFT**

**Figure 2.** Dominant  $s$  channel  $b + \bar{b}$  (and  $\tau + \bar{\tau}$ ) production

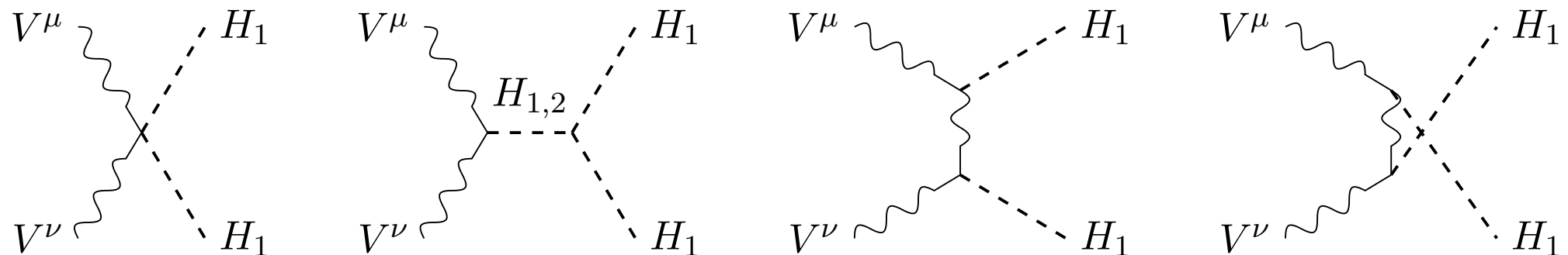


**Figure 3.** Dominant  $s/t$ -channel production of  $H_1$ s that decay dominantly to  $b + \bar{b}$

# Importance of VDM with Dark Higgs Boson

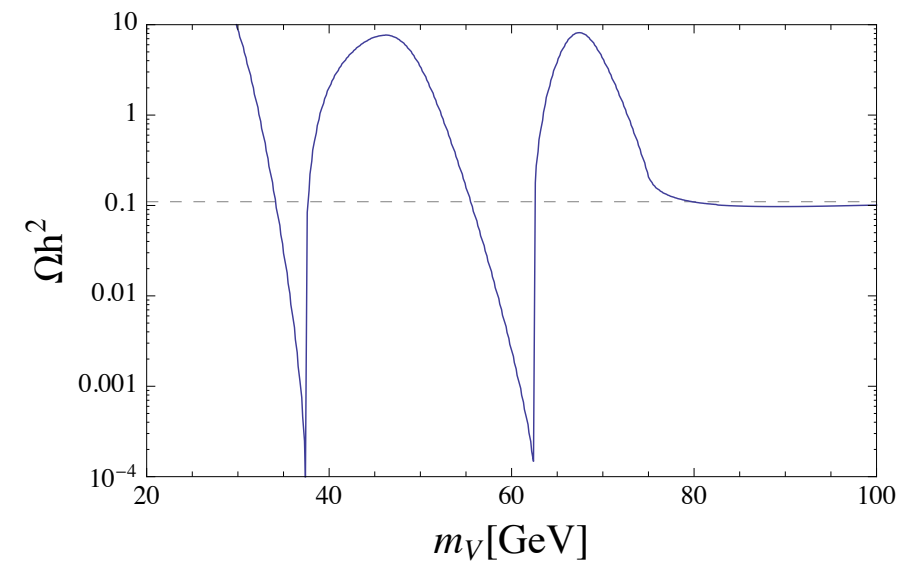


**Figure 4.** Relic density of dark matter as function of  $m_\psi$  for  $m_h = 125$ ,  $m_\phi = 75$  GeV,  $g_X = 0.2$ , and  $\alpha = 0.1$ .

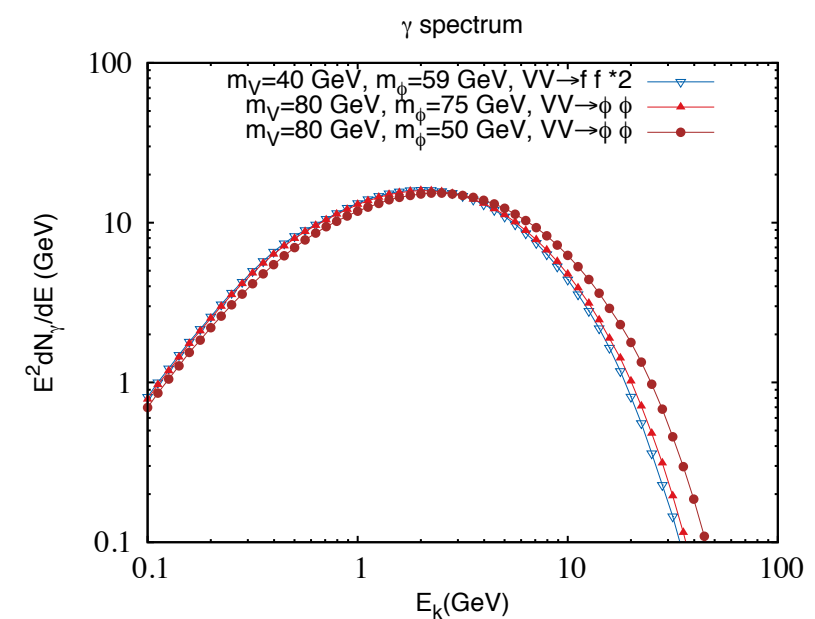
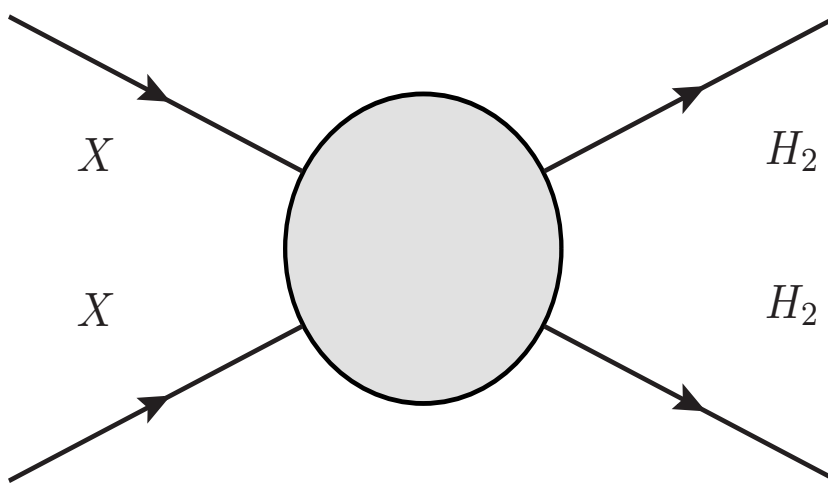


**Figure 5.** Illustration of  $\gamma$  spectra from different channels. The first two cases give almost the same spectra while in the third case  $\gamma$  is boosted so the spectrum is shifted to higher energy.

This mass range of VDM would have been  
impossible in the VDM model (EFT)

And No 2nd neutral scalar (Dark Higgs) in EFT



P.Ko, Yong Tang.  
arXiv:1504.03908

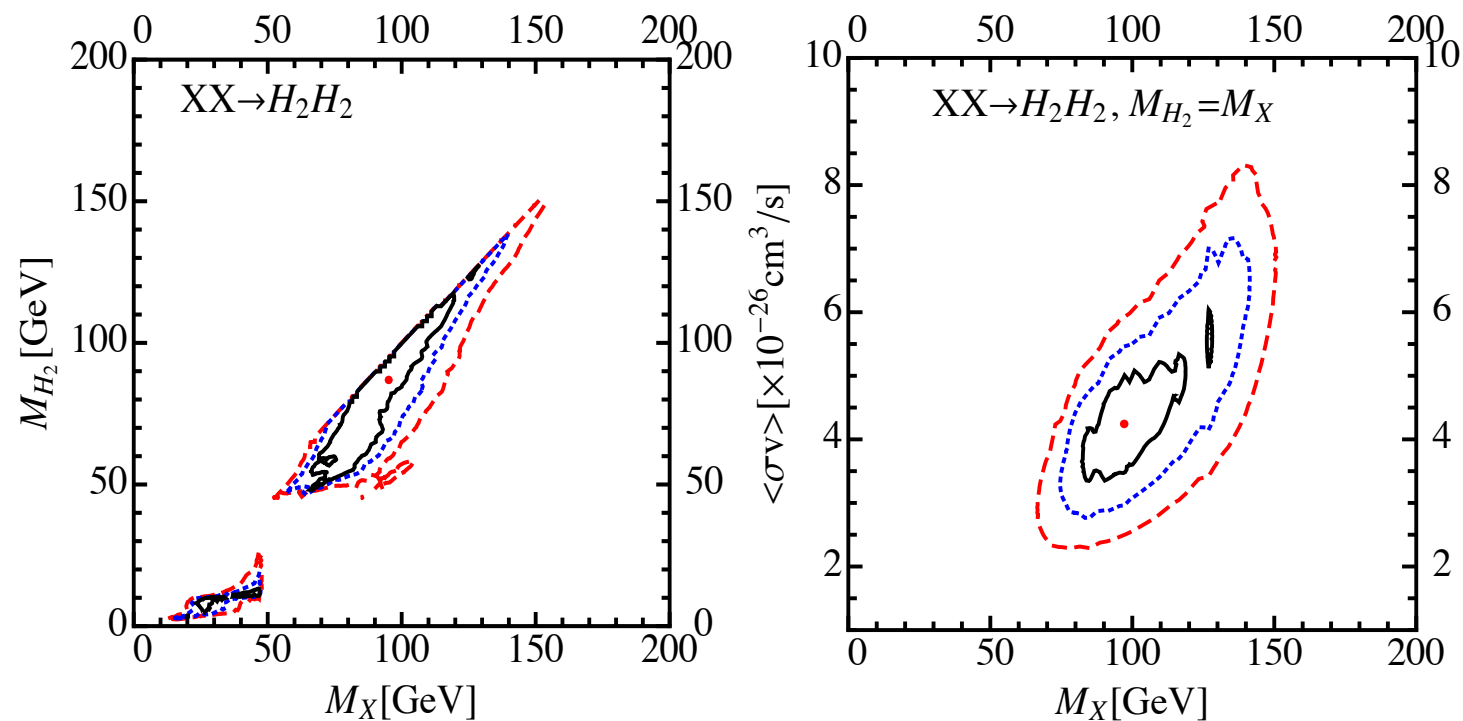


FIG. 3: The regions inside solid(black), dashed(blue) and long-dashed(red) contours correspond to  $1\sigma$ ,  $2\sigma$  and  $3\sigma$ , respectively. The red dots inside  $1\sigma$  contours are the best-fit points. In the left panel, we vary freely  $M_X$ ,  $M_{H_2}$  and  $\langle \sigma v \rangle$ . While in the right panel, we fix the mass of  $H_2$ ,  $M_{H_2} \simeq M_X$ .

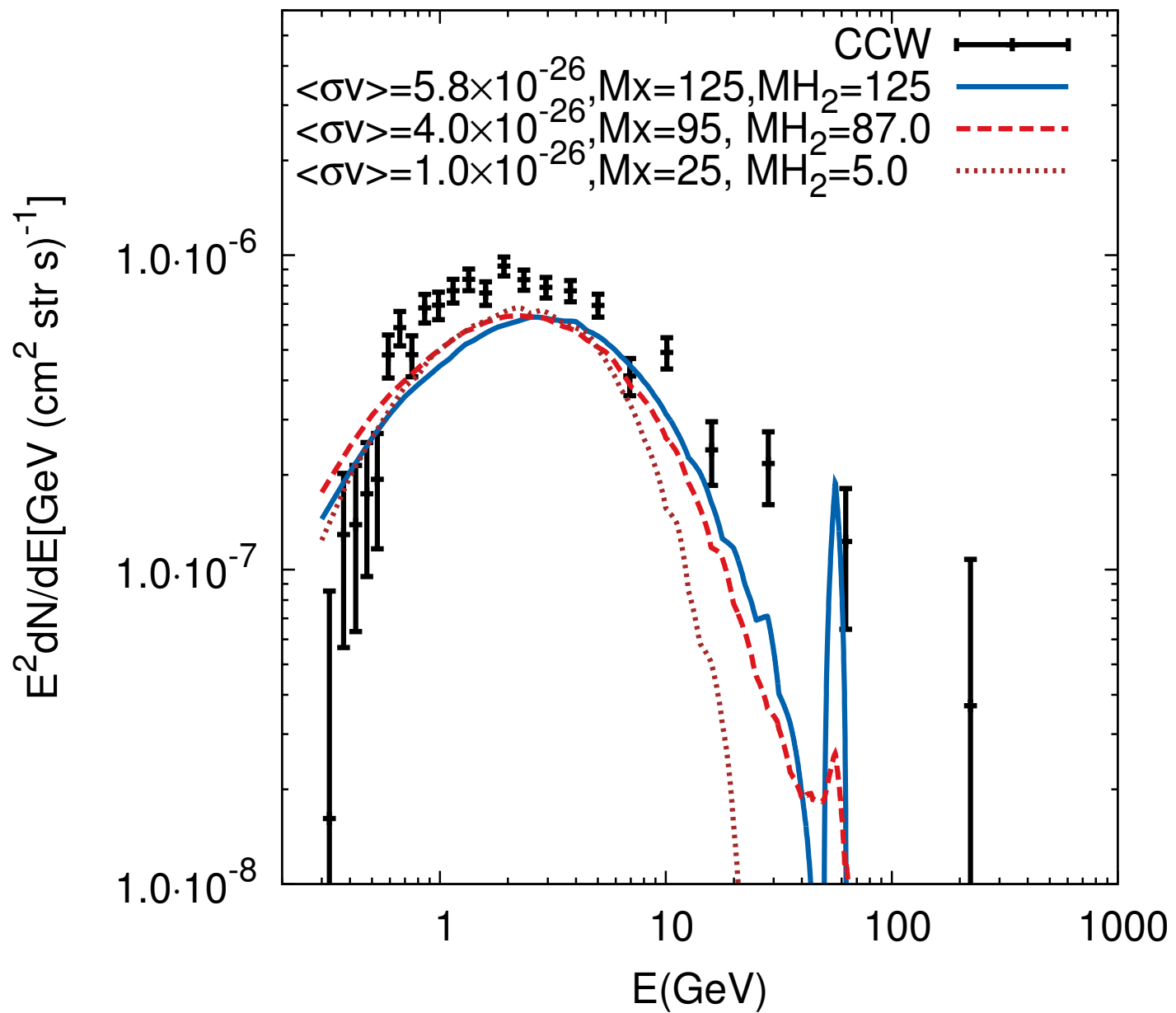


FIG. 2: Three illustrative cases for gamma-ray spectra in contrast with CCW data points [11]. All masses are in GeV unit and  $\sigma v$  with  $\text{cm}^3/\text{s}$ . Line shape around  $E \simeq M_{H_2}/2$  is due to decay modes,  $H_2 \rightarrow \gamma\gamma, Z\gamma$ .

# This would have never been possible within the DM EFT

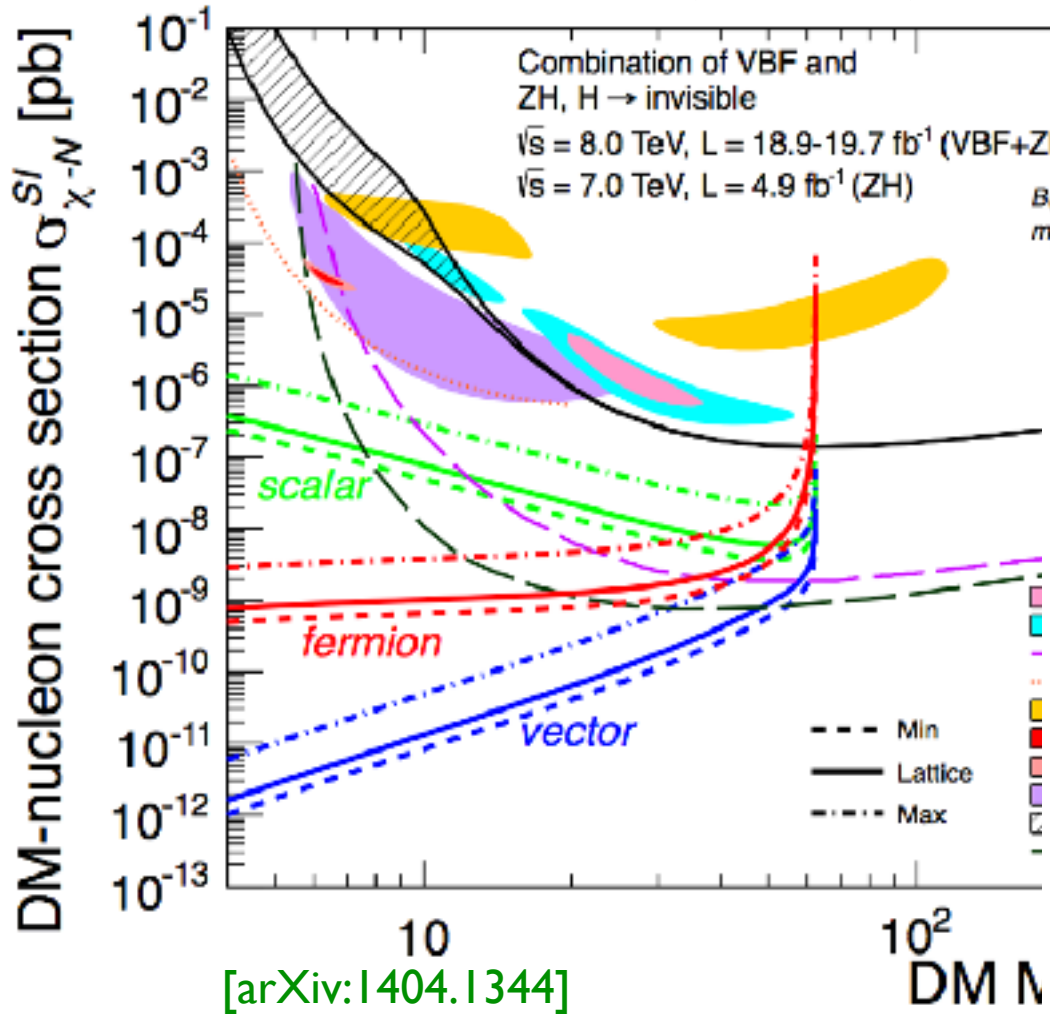
P.Ko, Yong Tang.  
arXiv:1504.03908

Channels	Best-fit parameters	$\chi^2_{\min}/\text{d.o.f.}$	$p$ -value
$XX \rightarrow H_2H_2$ (with $M_{H_2} \neq M_X$ )	$M_X \simeq 95.0\text{GeV}$ , $M_{H_2} \simeq 86.7\text{GeV}$ $\langle\sigma v\rangle \simeq 4.0 \times 10^{-26}\text{cm}^3/\text{s}$	22.0/21	0.40
$XX \rightarrow H_2H_2$ (with $M_{H_2} = M_X$ )	$M_X \simeq 97.1\text{GeV}$ $\langle\sigma v\rangle \simeq 4.2 \times 10^{-26}\text{cm}^3/\text{s}$	22.5/22	0.43
$XX \rightarrow H_1H_1$ (with $M_{H_1} = 125\text{GeV}$ )	$M_X \simeq 125\text{GeV}$ $\langle\sigma v\rangle \simeq 5.5 \times 10^{-26}\text{cm}^3/\text{s}$	24.8/22	0.30
$XX \rightarrow b\bar{b}$	$M_X \simeq 49.4\text{GeV}$ $\langle\sigma v\rangle \simeq 1.75 \times 10^{-26}\text{cm}^3/\text{s}$	24.4/22	0.34

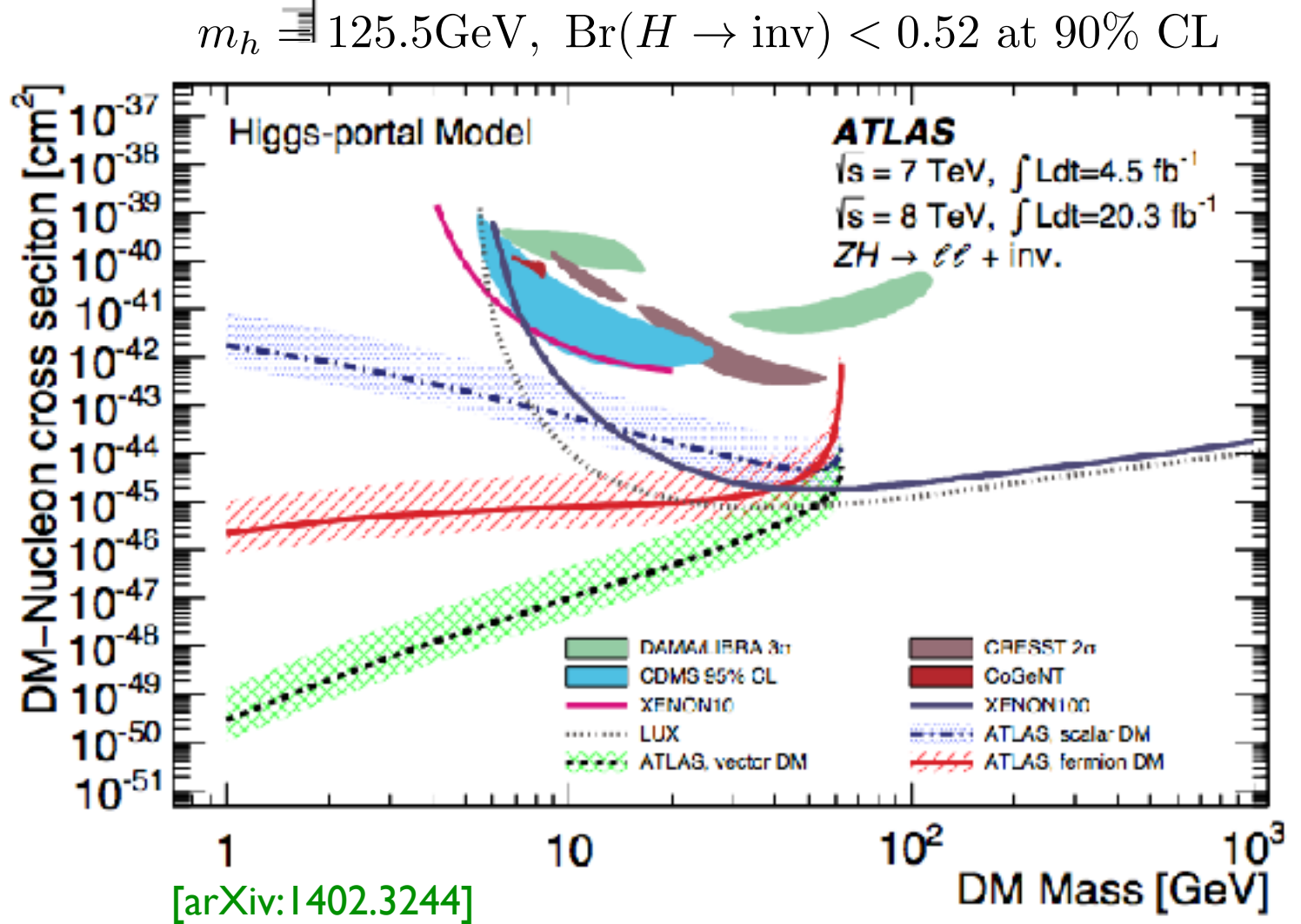
TABLE I: Summary table for the best fits with three different assumptions.

# Collider Implications

$m_h = 125\text{GeV}$ ,  $\text{Br}(H \rightarrow \text{inv}) < 0.51$  at 90% CL



Based on EFTs



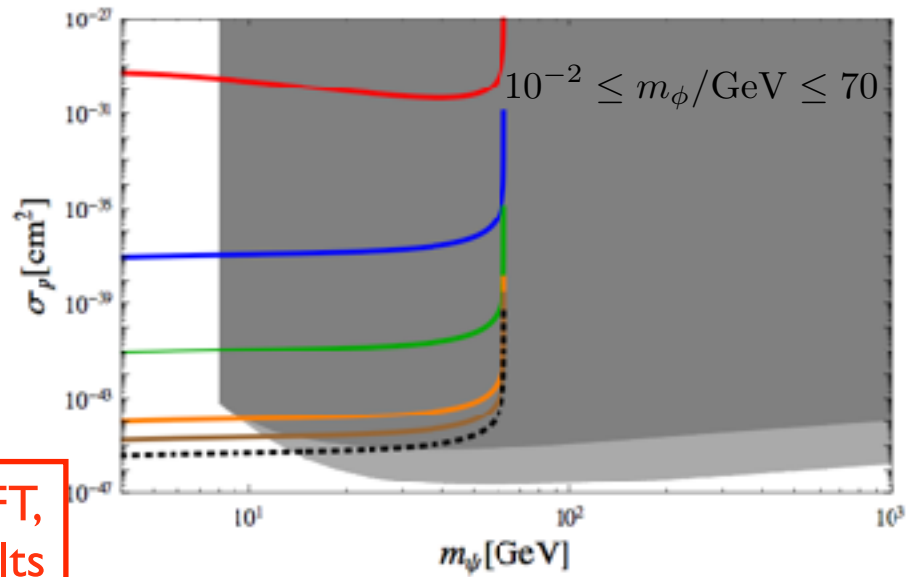
- However, in renormalizable unitary models of Higgs portals, 2 more relevant parameters

$$\begin{aligned}\mathcal{L}_{\text{SFDM}} = & \bar{\psi} (i\partial - m_\psi - \lambda_\psi S) - \mu_{HS} S H^\dagger H - \frac{\lambda_{HS}}{2} S^2 H^\dagger H \\ & + \frac{1}{2} \partial_\mu S \partial^\mu S - \frac{1}{2} m_S^2 S^2 - \mu_S^3 S - \frac{\mu_S'}{3} S^3 - \frac{\lambda_S}{4} S^4.\end{aligned}$$

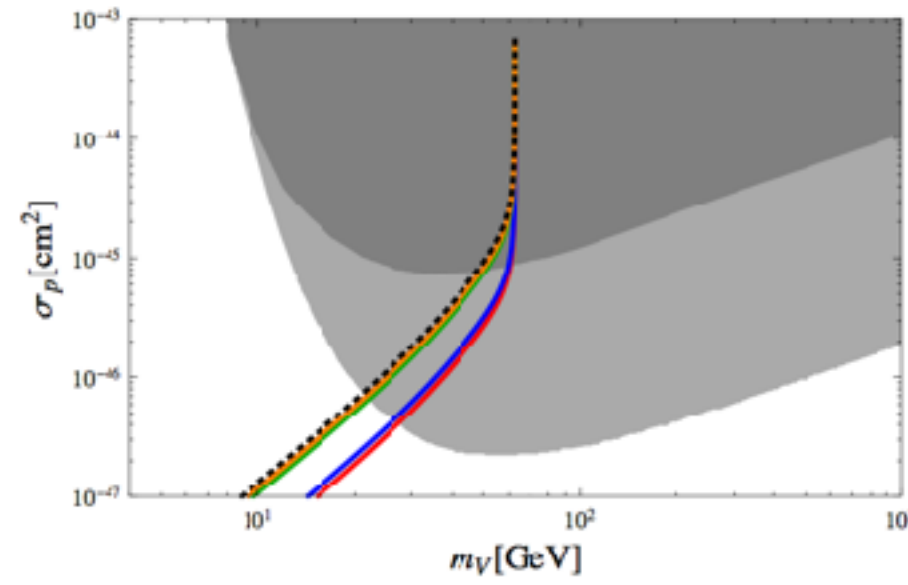
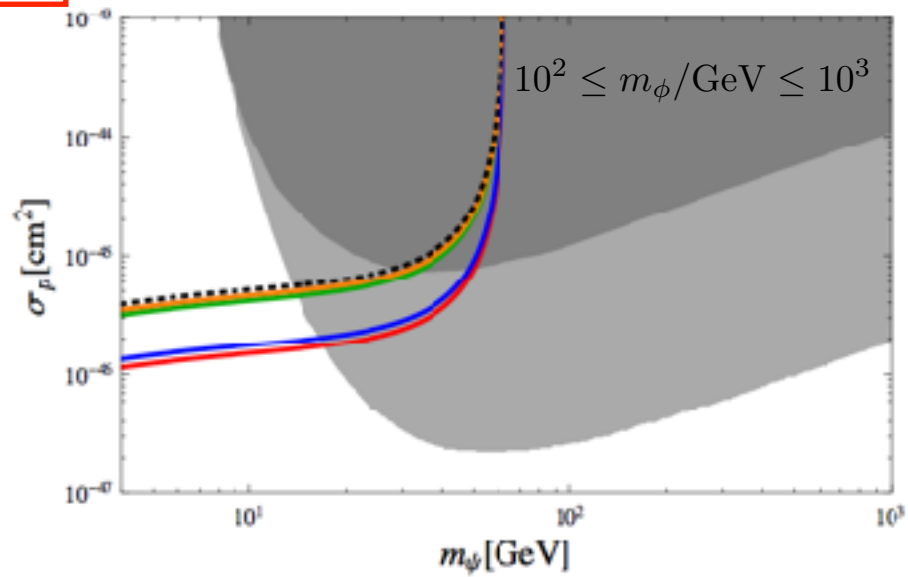
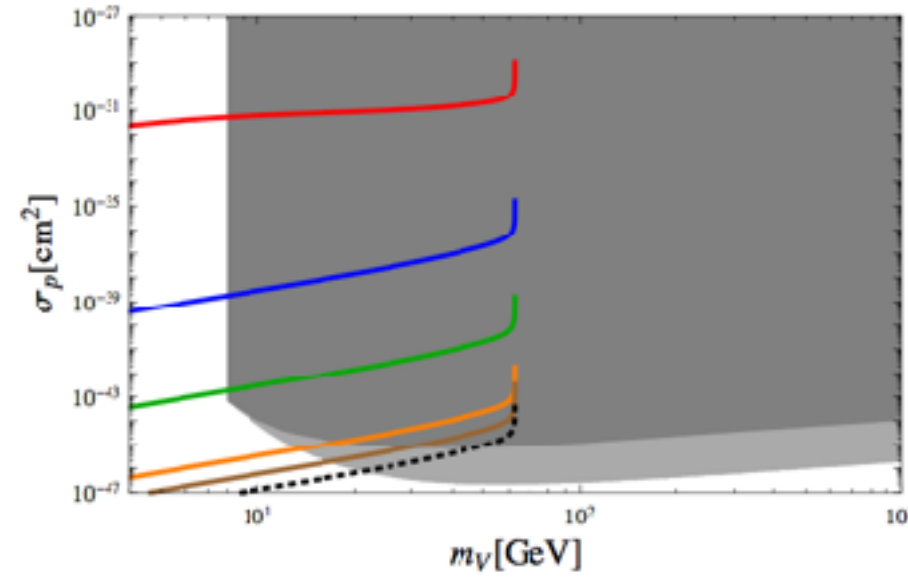
[arXiv: 1405.3530, S. Baek, P. Ko & WIPark, PRD]

$$\begin{aligned}\sigma_p^{\text{SI}} &= (\sigma_p^{\text{SI}})_{\text{EFT}} c_\alpha^4 m_h^4 \mathcal{F}(m_{\text{DM}}, \{m_i\}, v) \\ &\simeq (\sigma_p^{\text{SI}})_{\text{EFT}} c_\alpha^4 \left(1 - \frac{m_h^2}{m_2^2}\right)^2\end{aligned}$$

$$\mathcal{L}_{\text{VDM}} = -\frac{1}{4} V_{\mu\nu} V^{\mu\nu} + D_\mu \Phi^\dagger D^\mu \Phi - \lambda_\Phi \left(\Phi^\dagger \Phi - \frac{v_\Phi^2}{2}\right)^2 - \lambda_{\Phi H} \left(\Phi^\dagger \Phi - \frac{v_\Phi^2}{2}\right) \left(H^\dagger H - \frac{v_H^2}{2}\right)$$



Dashed curves: EFT,  
ATLAS, CMS results

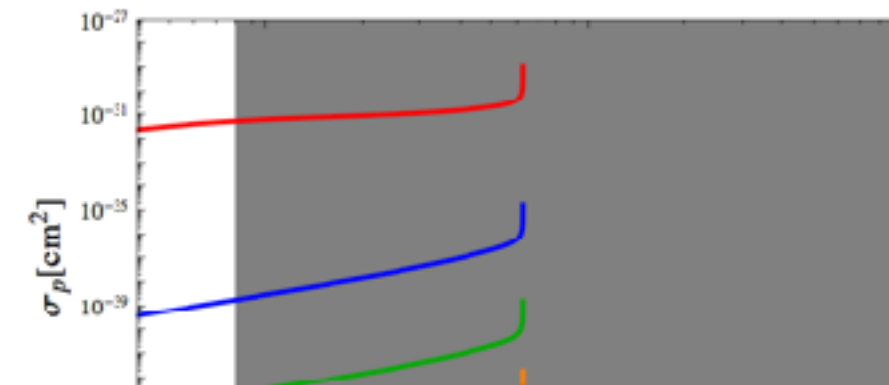
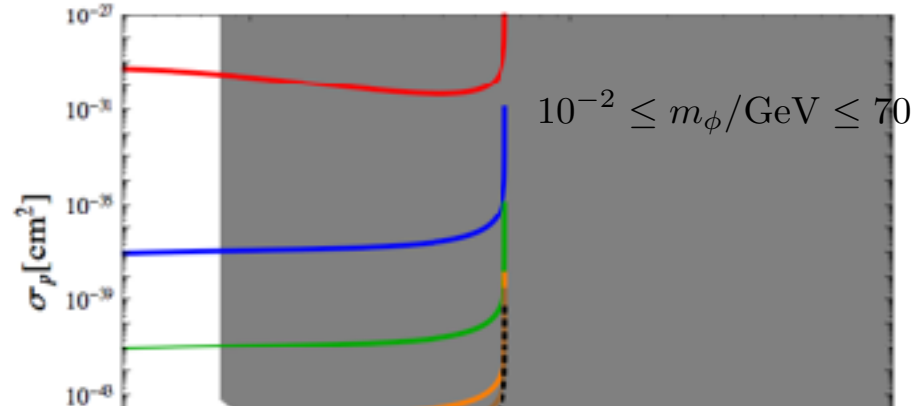


- However, in renormalizable unitary models of Higgs portals, **2 more relevant parameters**

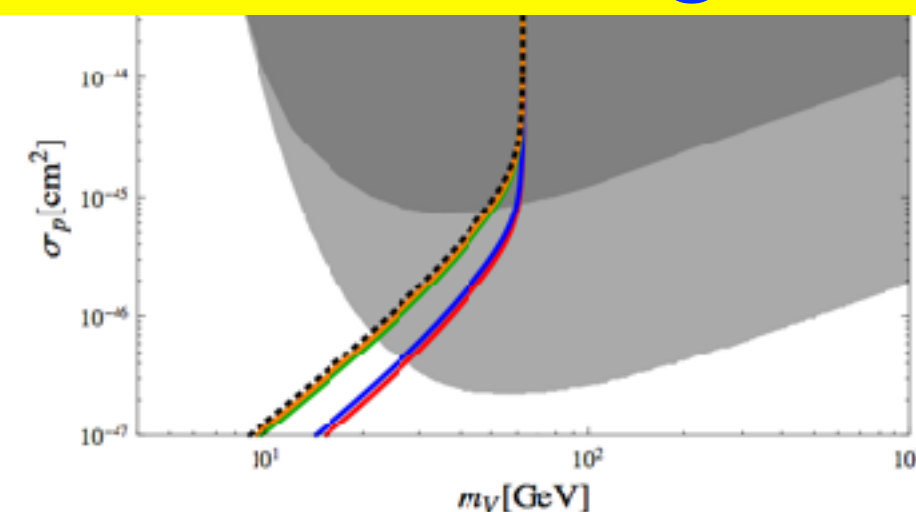
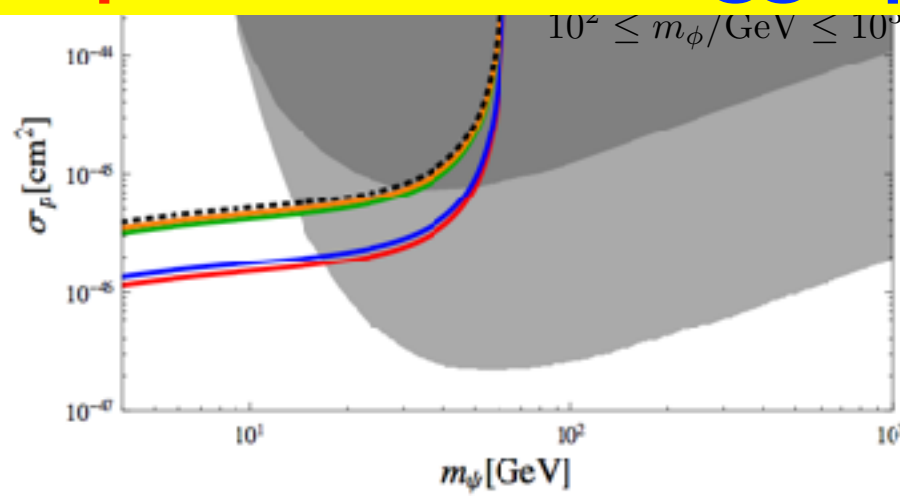
$$\begin{aligned}\mathcal{L}_{\text{SFDM}} = & \bar{\psi} (i\partial - m_\psi - \lambda_\psi S) - \mu_{HS} S H^\dagger H - \frac{\lambda_{HS}}{2} S^2 H^\dagger H \\ & + \frac{1}{2} \partial_\mu S \partial^\mu S - \frac{1}{2} m_S^2 S^2 - \mu_S^3 S - \frac{\mu_S'}{3} S^3 - \frac{\lambda_S}{4} S^4.\end{aligned}$$

$$\begin{aligned}\sigma_p^{\text{SI}} = & (\sigma_p^{\text{SI}})_{\text{EFT}} c_\alpha^4 m_h^4 \mathcal{F}(m_{\text{DM}}, \{m_i\}, v) \\ \simeq & (\sigma_p^{\text{SI}})_{\text{EFT}} c_\alpha^4 \left(1 - \frac{m_h^2}{m_2^2}\right)^2\end{aligned}$$

$$\mathcal{L}_{\text{VDM}} = -\frac{1}{4} V_{\mu\nu} V^{\mu\nu} + D_\mu \Phi^\dagger D^\mu \Phi - \lambda_\Phi \left(\Phi^\dagger \Phi - \frac{v_\Phi^2}{2}\right)^2 - \lambda_{\Phi H} \left(\Phi^\dagger \Phi - \frac{v_\Phi^2}{2}\right) \left(H^\dagger H - \frac{v_H^2}{2}\right)$$



Interpretation of collider data is **quite model-dependent** in Higgs portal DMs and in general



# Invisible H decay into a pair of VDM

[arXiv: 1405.3530, S. Baek, P. Ko & WIPark, PRD]

$$(\Gamma_h^{\text{inv}})_{\text{EFT}} = \frac{\lambda_{VH}^2}{128\pi} \frac{v_H^2 m_h^3}{m_V^4} \times \left(1 - \frac{4m_V^2}{m_h^2} + 12 \frac{m_V^4}{m_h^4}\right) \left(1 - \frac{4m_V^2}{m_h^2}\right)^{1/2} \quad (23)$$

VS.

$$\Gamma_i^{\text{inv}} = \frac{g_X^2}{32\pi} \frac{m_i^3}{m_V^2} \left(1 - \frac{4m_V^2}{m_i^2} + 12 \frac{m_V^4}{m_i^4}\right) \left(1 - \frac{4m_V^2}{m_i^2}\right)^{1/2} \sin^2 \alpha \quad (22)$$

Invisible H decay width : finite for small m<sub>V</sub>  
in unitary/renormalizable model

# DD vs. Monojet : Why complementarity breaks down in EFT ?

- S. Baek, P. Ko, M. Park, WIPark, C.Yu, arXiv:1506.06556  
Phys. Lett. B756 (2016)289
- P. Ko and Jinmian Li, arXiv:1610.03997, PLB (2017)

# Why is it broken down in DM EFT ?

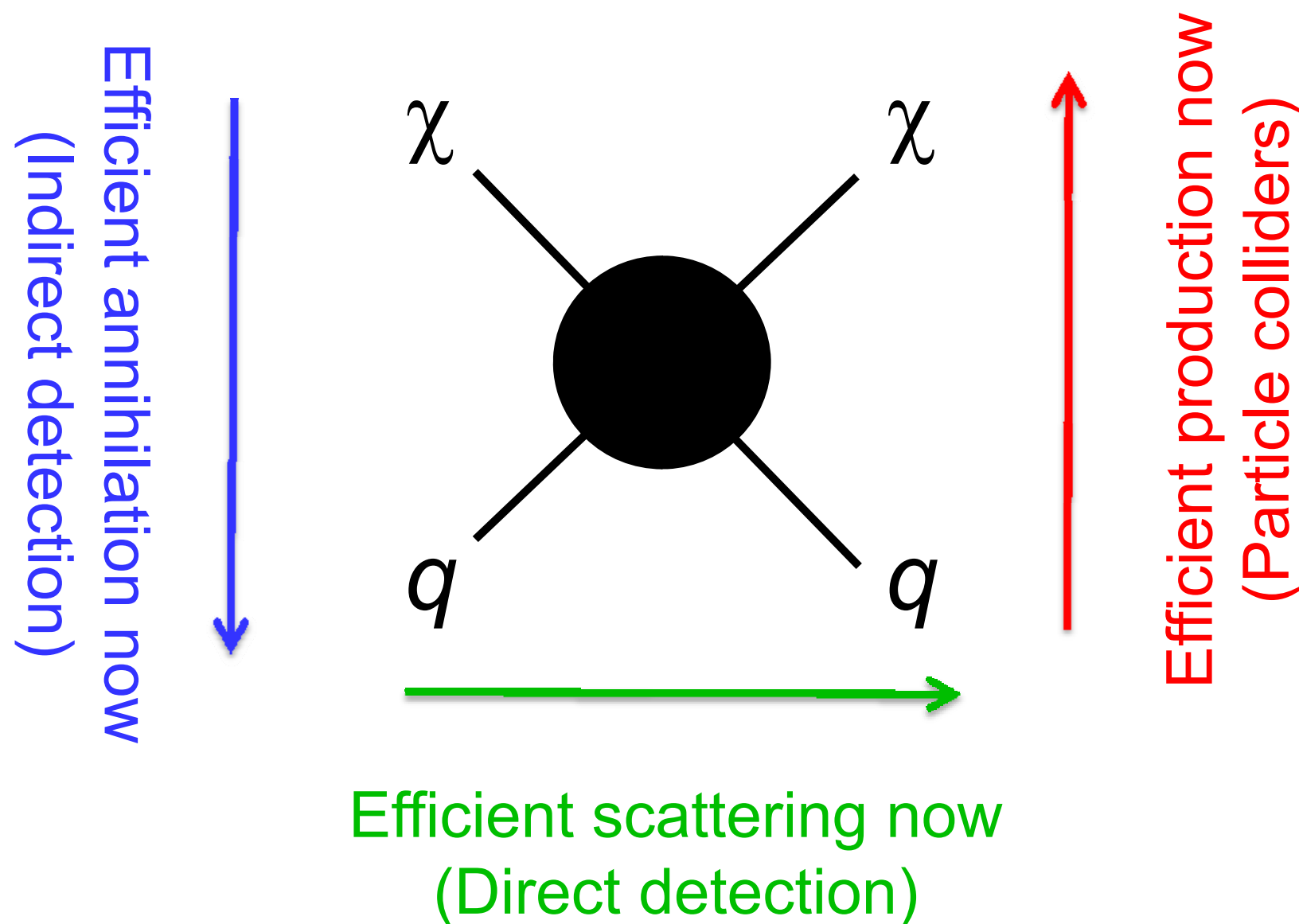
The most nontrivial example is  
the (scalar)x(scalar) operator  
for DM-N scattering

$$\mathcal{L}_{SS} \equiv \frac{1}{\Lambda_{dd}^2} \bar{q} q \bar{\chi} \chi \quad \text{or} \quad \frac{m_q}{\Lambda_{dd}^3} \bar{q} q \bar{\chi} \chi$$

This operator clearly violates  
the SM gauge symmetry, and  
we have to fix this problem

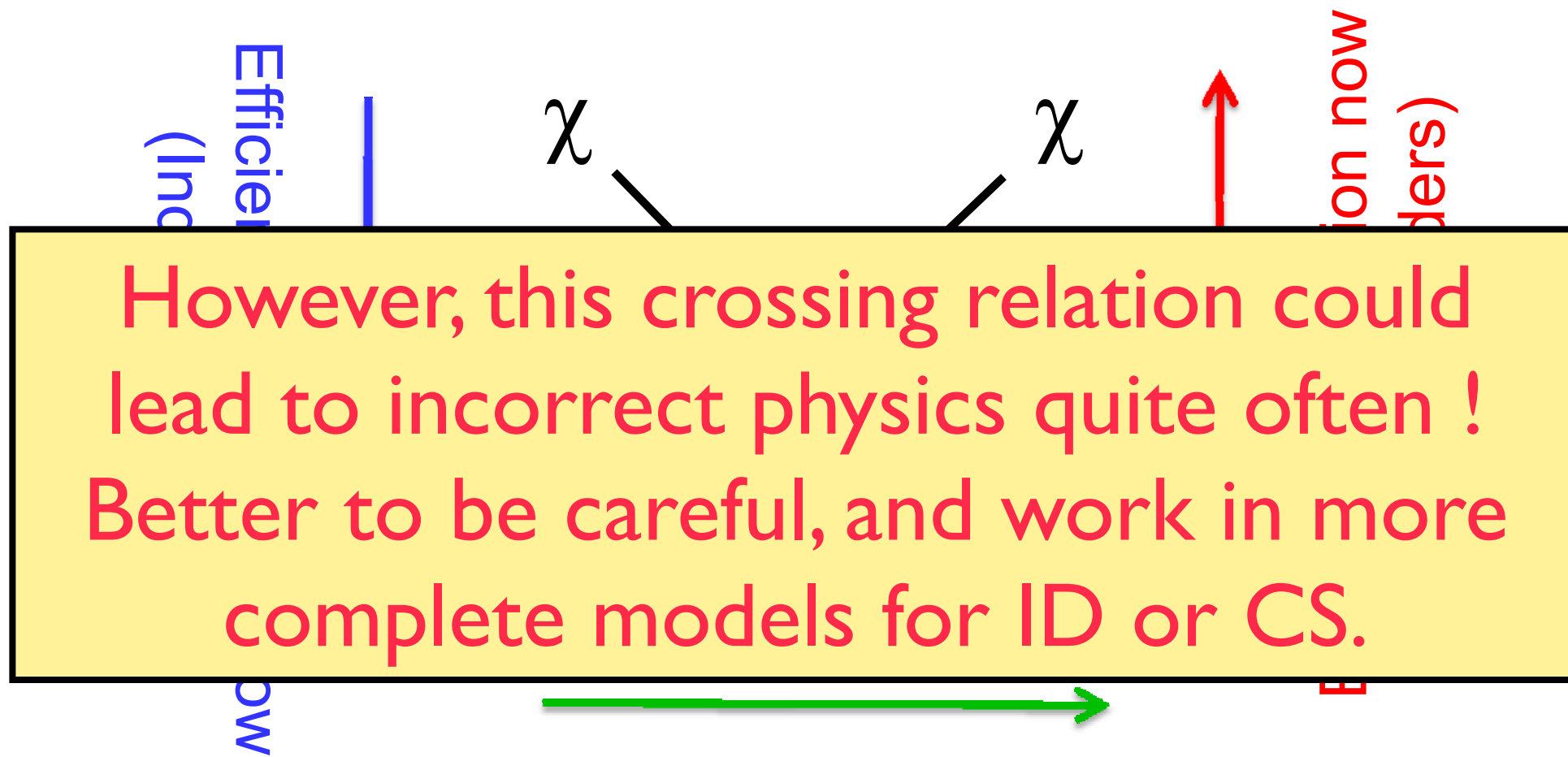
# Crossing & WIMP detection

Correct relic density → Efficient annihilation then



# Crossing & WIMP detection

Correct relic density → Efficient annihilation then



Efficient scattering now  
(Direct detection)

# From Paolo Gondolo's talk

## Effective operators: LHC & direct detection

Name	Operator	Coefficient
D1	$\bar{\chi}\chi\bar{q}q$	$m_q/M_*^3$
D2	$\bar{\chi}\gamma^5\chi\bar{q}q$	$im_q/M_*^3$
D3	$\bar{\chi}\chi\bar{q}\gamma^5q$	$im_q/M_*^3$
D4	$\bar{\chi}\gamma^5\chi\bar{q}\gamma^5q$	$m_q/M_*^3$
D5	$\bar{\chi}\gamma^\mu\chi\bar{q}\gamma_\mu q$	$1/M_*^2$
D6	$\bar{\chi}\gamma^\mu\gamma^5\chi\bar{q}\gamma_\mu q$	$1/M_*^2$
D7	$\bar{\chi}\gamma^\mu\chi\bar{q}\gamma_\mu\gamma^5q$	$1/M_*^2$
D8	$\bar{\chi}\gamma^\mu\gamma^5\chi\bar{q}\gamma_\mu\gamma^5q$	$1/M_*^2$
D9	$\bar{\chi}\sigma^{\mu\nu}\chi\bar{q}\sigma_{\mu\nu}q$	$1/M_*^2$
D10	$\bar{\chi}\sigma_{\mu\nu}\gamma^5\chi\bar{q}\sigma_{\alpha\beta}q$	$i/M_*^2$
D11	$\bar{\chi}\chi G_{\mu\nu}G^{\mu\nu}$	$\alpha_s/4M_*^3$
D12	$\bar{\chi}\gamma^5\chi G_{\mu\nu}G^{\mu\nu}$	$i\alpha_s/4M_*^3$
D13	$\bar{\chi}\chi G_{\mu\nu}\tilde{G}^{\mu\nu}$	$i\alpha_s/4M_*^3$
D14	$\bar{\chi}\gamma^5\chi G_{\mu\nu}\tilde{G}^{\mu\nu}$	$\alpha_s/4M_*^3$

Name	Operator	Coefficient
C1	$\chi^\dagger\chi\bar{q}q$	$m_q/M_*^2$
C2	$\chi^\dagger\chi\bar{q}\gamma^5q$	$im_q/M_*^2$
C3	$\chi^\dagger\partial_\mu\chi\bar{q}\gamma^\mu q$	$1/M_*^2$
C4	$\chi^\dagger\partial_\mu\chi\bar{q}\gamma^\mu\gamma^5q$	$1/M_*^2$
C5	$\chi^\dagger\chi G_{\mu\nu}G^{\mu\nu}$	$\alpha_s/4M_*^2$
C6	$\chi^\dagger\chi G_{\mu\nu}\tilde{G}^{\mu\nu}$	$i\alpha_s/4M_*^2$
R1	$\chi^2\bar{q}q$	$m_q/2M_*^2$
R2	$\chi^2\bar{q}\gamma^5q$	$im_q/2M_*^2$
R3	$\chi^2 G_{\mu\nu}G^{\mu\nu}$	$\alpha_s/8M_*^2$
R4	$\chi^2 G_{\mu\nu}\tilde{G}^{\mu\nu}$	$i\alpha_s/8M_*^2$

Table of effective operators relevant for the  
collider/direct detection connection

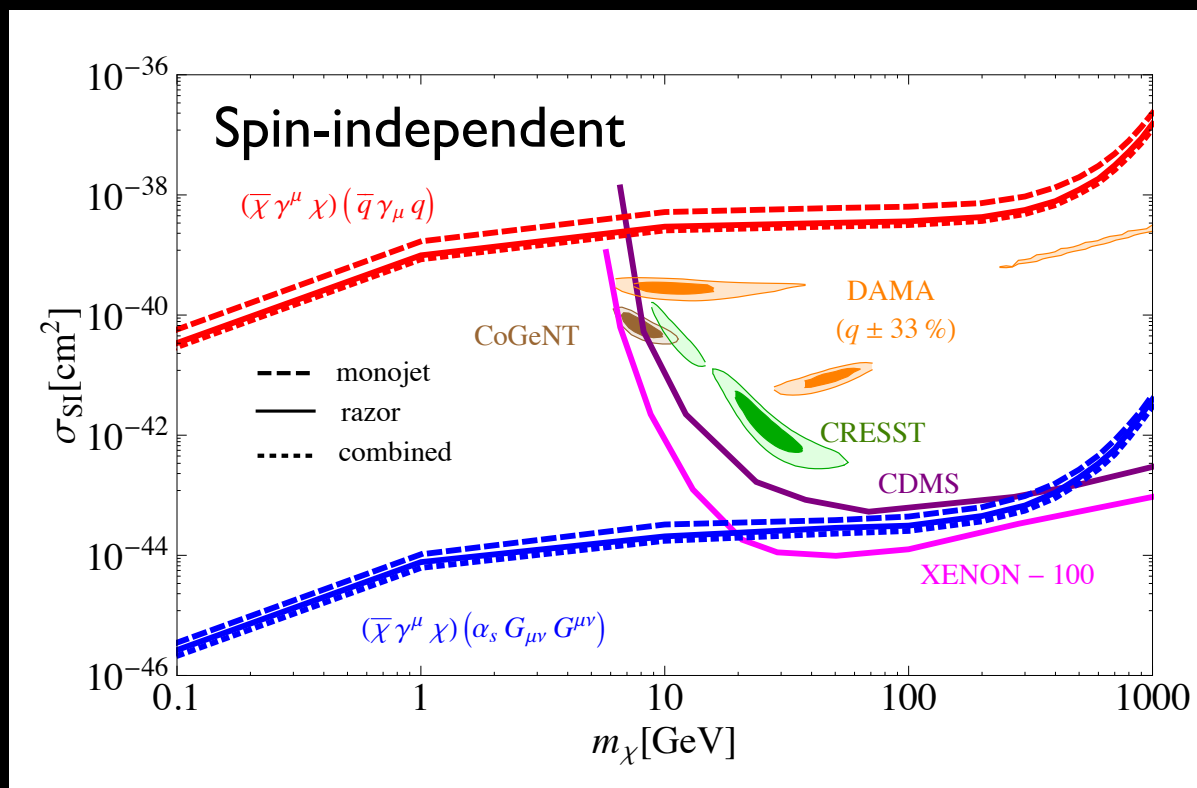
Goodman, Ibe, Rajaraman, Shepherd, Tait, Yu 2010

# From Paolo Gondolo's talk

## Effective operators: LHC & direct detection

LHC limits on WIMP-quark and WIMP-gluon interactions  
are competitive with direct searches

Beltran et al, Agrawal et al., Goodman et al., Bai et al., 2010; Goodman et al., Rajaraman et al. Fox et al., 2011; Cheung et al., Fitzpatrick et al., March-Russel et al., Fox et al., 2012.....



*These bounds do not apply to SUSY, etc.*

*Complete theories contain sums of operators (interference) and not-so-heavy mediators (Higgs)*

Fox, Harnik, Primulando, Yu 2012

# Limitation and Proposal

- EFT is good for direct detection, but not for indirect or collider searches as well as thermal relic density calculations in general
- Issues : **Violation of Unitarity and SM gauge invariance**, Identifying the relevant dynamical fields at energy scale we are interested in, Symmetry stabilizing DM etc.

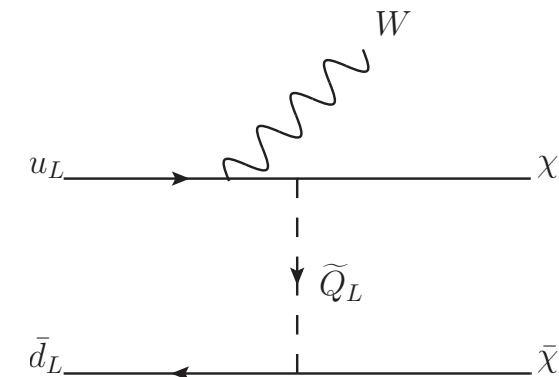
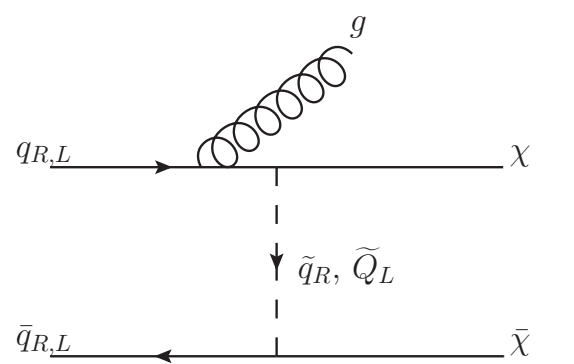
$$\frac{1}{\Lambda_i^2} \bar{q}\Gamma_i q \bar{\chi}\Gamma_i \chi \rightarrow \frac{g_q g_\chi}{m_\phi^2 - s} \bar{q}\Gamma_i q \bar{\chi}\Gamma_i \chi$$

- Usually effective operator is replaced by a single propagator in simplified DM models
- This is not good enough, since we have to respect the full SM gauge symmetry (Bell et al for W+missing ET)
- In general we need two propagators, not one propagator, because there are two independent chiral fermions in 4-dim spacetime

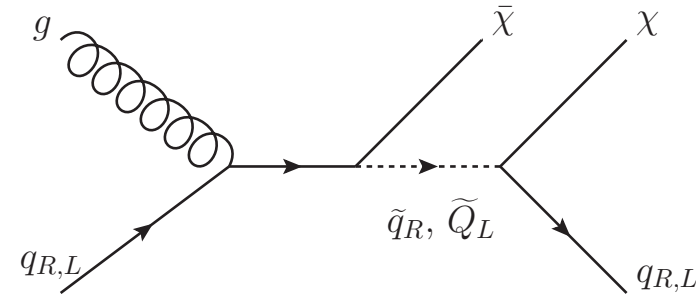
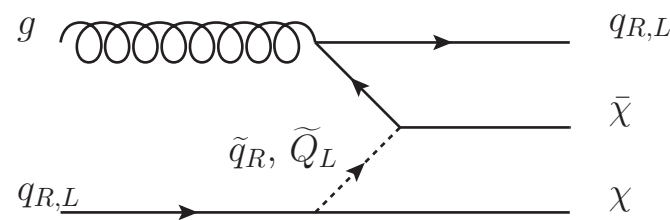
arXiv:1605.07058 (with A. Natale, M. Park, H. Yokoya)

## for t-channel mediator

Our Model: a 'simplified model' of colored  $t$ -channel, spin-0, mediators which produce various mono- $x$  + missing energy signatures (mono-Jet, mono-W, mono-Z, etc.):



**W+missing ET : special**



$$\frac{1}{\Lambda_i^2} \bar{q}\Gamma_i q \bar{\chi}\Gamma_i \chi \rightarrow \frac{g_q g_\chi}{m_\phi^2 - s} \bar{q}\Gamma_i q \bar{\chi}\Gamma_i \chi$$

- This is good only for W+missing ET, and not for other signatures
- The same is also true for **(scalar)x(scalar) operator, and** lots of confusion on this operator in literature
- Therefore let me concentrate on this case in detail in this talk

$$\bar{Q}_L H d_R \quad \text{or} \quad \bar{Q}_L \tilde{H} u_R, \quad \text{OK}$$

$$h\bar{\chi}\chi, \quad s\bar{q}q$$

Both break SM gauge

$$\begin{aligned} \mathcal{L} &= \frac{1}{2}m_S^2 S^2 - \lambda_{s\chi}s\bar{\chi}\chi - \lambda_{sq}s\bar{q}q \\ \mathcal{L} &= -\lambda_{h\chi}h\bar{\chi}\chi - \lambda_{hq}h\bar{q}q \end{aligned}$$

Therefore these Lagragians  
are not good enough

$$s\bar{\chi}\chi \times h\bar{q}q \rightarrow \frac{1}{m_s^2}\bar{\chi}\chi\bar{q}q$$

Need the mixing between s and h

# Full Theory Calculation

$$\chi(p) + q(k) \rightarrow \chi(p') + q(k')$$

$$\begin{aligned}\mathcal{M} &= \overline{u(p')} u(p) \overline{u(q')} u(q) \frac{m_q}{v} \lambda_s \sin \alpha \cos \alpha \left[ \frac{1}{t - m_{125}^2 + im_{125}\Gamma_{125}} - \frac{1}{t - m_2^2 + im_s\Gamma_2} \right] \\ &\rightarrow \overline{u(p')} u(p) \overline{u(q')} u(q) \frac{m_q}{2v} \lambda_s \sin 2\alpha \left[ \frac{1}{m_{125}^2} - \frac{1}{m_2^2} \right] \\ &\rightarrow \overline{u(p')} u(p) \overline{u(q')} u(q) \frac{m_q}{2v} \lambda_s \sin 2\alpha \frac{1}{m_{125}^2} \equiv \frac{m_q}{\Lambda_{dd}^3} \overline{u(p')} u(p) \overline{u(q')} u(q)\end{aligned}$$

$$\begin{aligned}\Lambda_{dd}^3 &\equiv \frac{2m_{125}^2 v}{\lambda_s \sin 2\alpha} \left( 1 - \frac{m_{125}^2}{m_2^2} \right)^{-1} \\ \bar{\Lambda}_{dd}^3 &\equiv \frac{2m_{125}^2 v}{\lambda_s \sin 2\alpha}\end{aligned}$$

# Monojet+missing ET

Can be obtained by crossing :  $s \leftrightarrow t$

$$\frac{1}{\Lambda_{dd}^3} \rightarrow \frac{1}{\Lambda_{dd}^3} \left[ \frac{m_{125}^2}{s - m_{125}^2 + im_{125}\Gamma_{125}} - \frac{m_{125}^2}{s - m_2^2 + im_2\Gamma_2} \right] = \frac{1}{\Lambda_{col}^3(s)}$$

There is no single scale you can define  
for collider search for missing ET

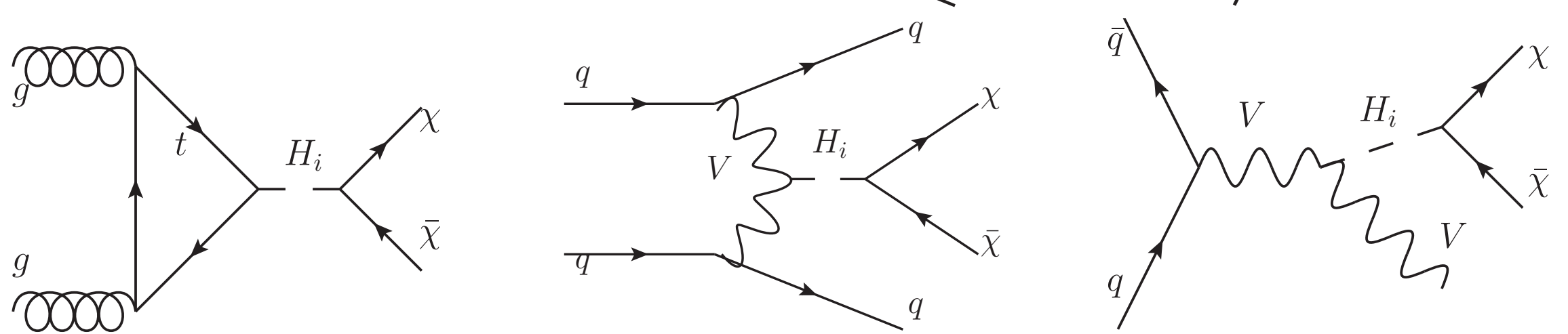


**Figure 1:** The dominant DM production processes at LHC.

Interference between 2 scalar bosons could  
be important in certain parameter regions

$$\frac{d\sigma_i}{dm_{\chi\chi}} \propto \left| \frac{\sin 2\alpha \ g_\chi}{m_{\chi\chi}^2 - m_{H_1}^2 + im_{H_1}\Gamma_{H_1}} - \frac{\sin 2\alpha \ g_\chi}{m_{\chi\chi}^2 - m_{H_2}^2 + im_{H_2}\Gamma_{H_2}} \right|^2$$

$$\sin \alpha = 0.2, g_\chi = 1, m_\chi = 80 \text{GeV}$$

# Interference effects

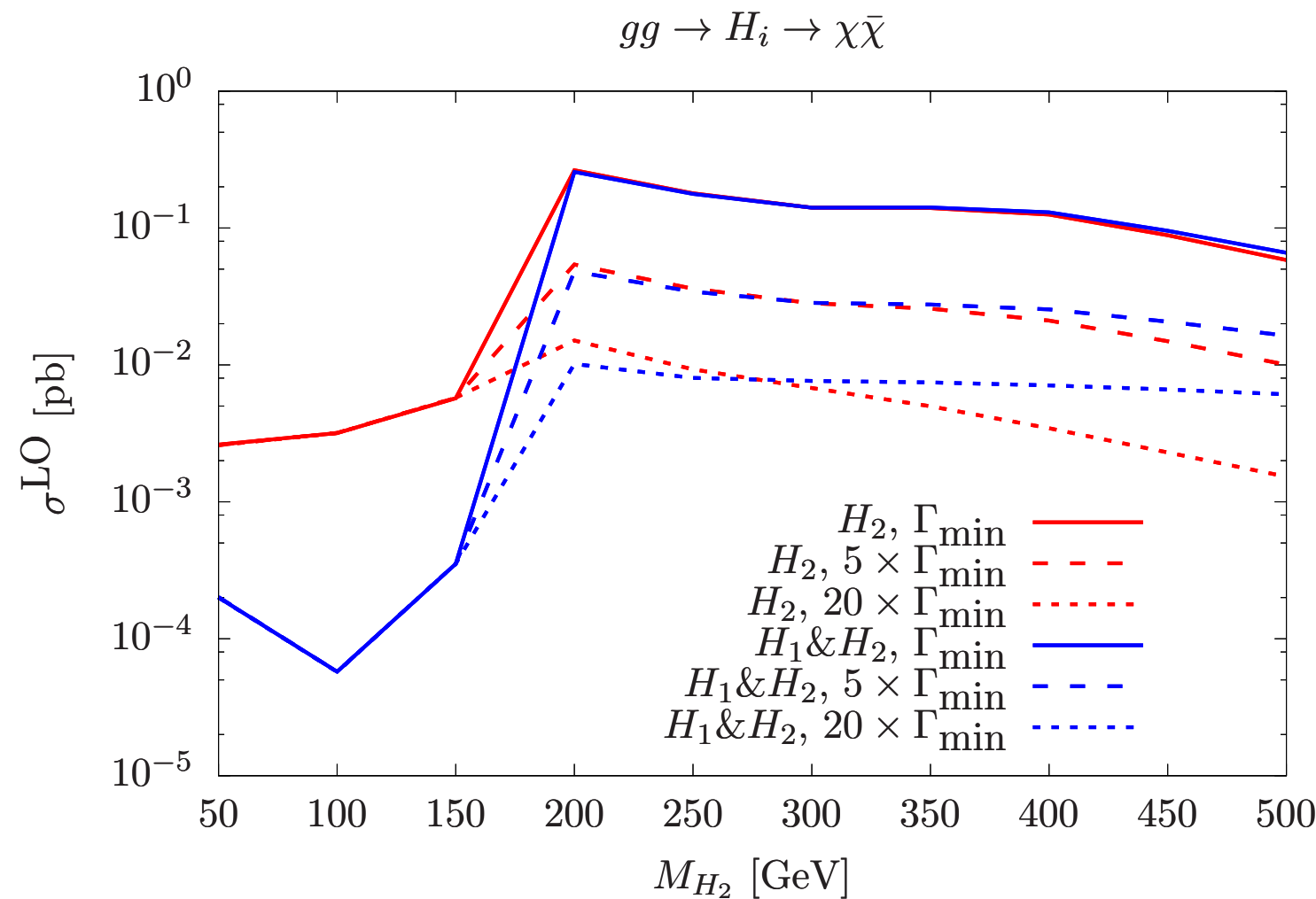


**Figure 2:** The LO cross section for gluon-gluon fusion process at 13 TeV LHC. The meanings of the different line types are explained in the text and the similar strategy will be used in all figures.

# Parton level distrib.

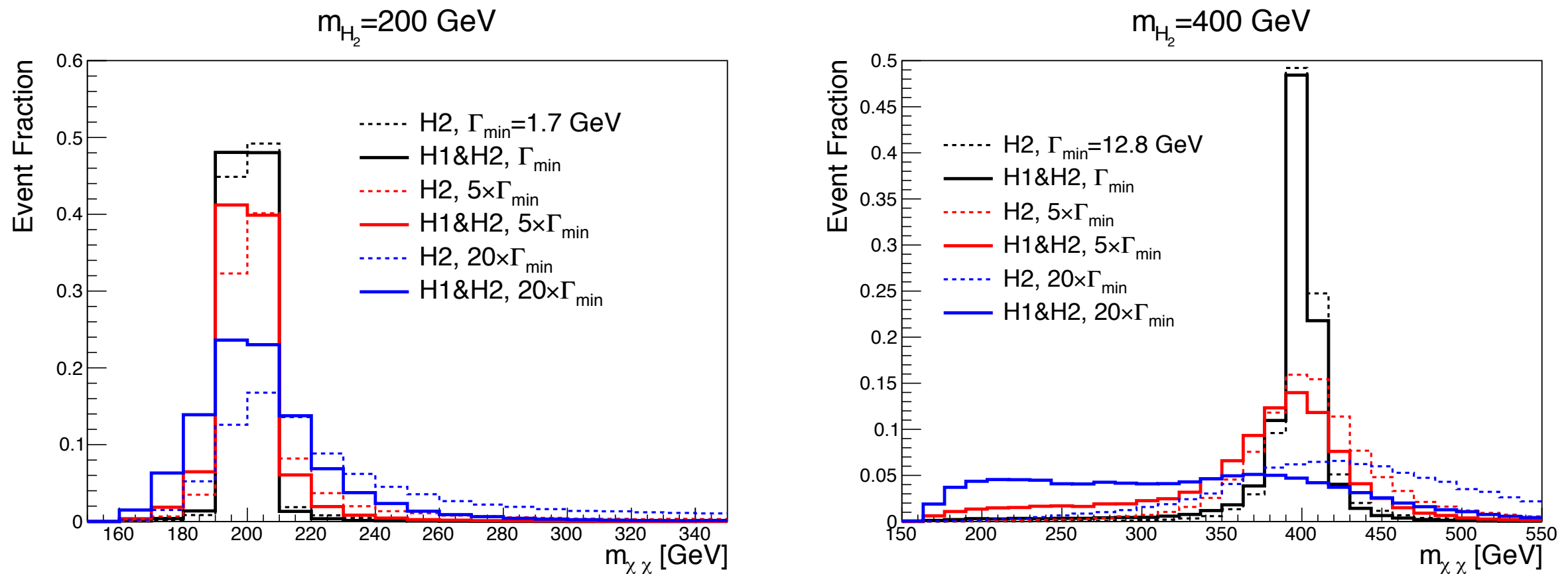


**Figure 3:** The parton level distributions of  $m_{\chi\bar{\chi}}$  for gluon-gluon fusion process at 13 TeV LHC.

# Exclusion limits with interference effects

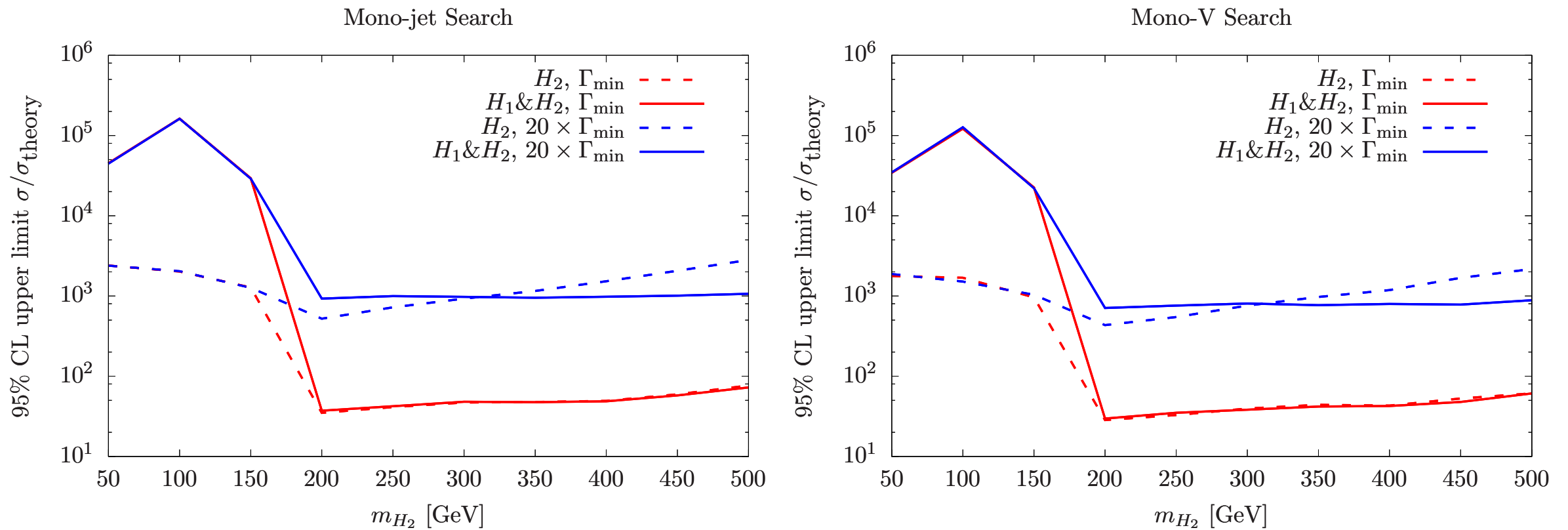


**Figure 8:** The CMS exclusion limits on our simplified models. Left: upper limit from mono-jet search. Right: upper limit from mono-V search.

- P. Ko and Jinmian Li, 1610.03997, PLB (2017)
- S. Baek, P. Ko and Jinmian Li, 1701.04131

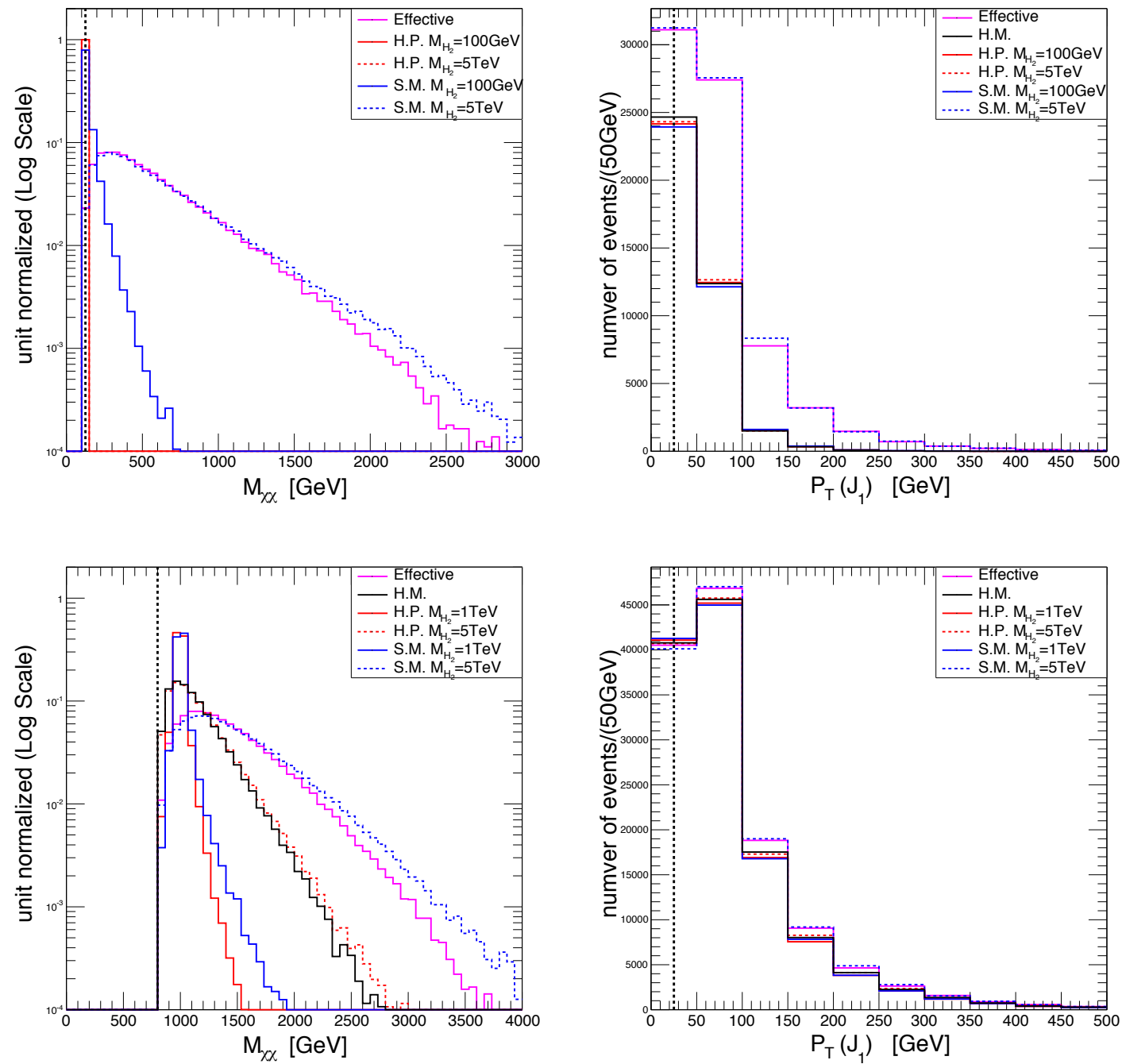


FIG. 1: In ATLAS 8TeV mono-jet+ $\cancel{E}_T$  search [6] we plot  $M_{\chi\chi}$  and the  $P_T$  of a hardest jet in a reconstruction level (after a detector simulation). Upper panels are with  $m_\chi = 50$  GeV and lower panels are of  $m_\chi = 400$  GeV.

- EFT : Effective operator  $\mathcal{L}_{int} = \frac{m_q}{\Lambda_{dd}^3} \bar{q} q \bar{\chi} \chi$
- S.M.: Simple scalar mediator  $S$  of  

$$\mathcal{L}_{int} = \left( \frac{m_q}{v_H} \sin \alpha \right) S \bar{q} q - \lambda_s \cos \alpha S \bar{\chi} \chi$$
- H.M.: A case where a Higgs is a mediator  

$$\mathcal{L}_{int} = - \left( \frac{m_q}{v_H} \cos \alpha \right) H \bar{q} q - \lambda_s \sin \alpha H \bar{\chi} \chi$$
- H.P.: Higgs portal model as in eq. (2).

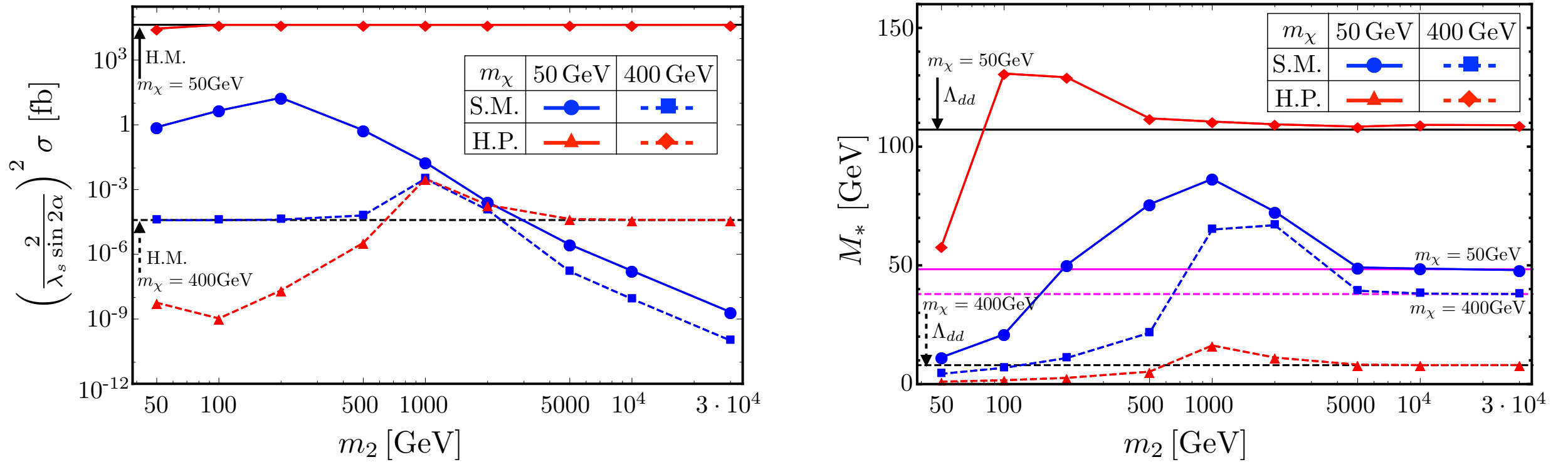


FIG. 1: We follow ATLAS 8TeV mono-jet+ $E_T$  searches [2]. For (a) we simulated various models for the

# $t\bar{T} + \text{missing ET}$

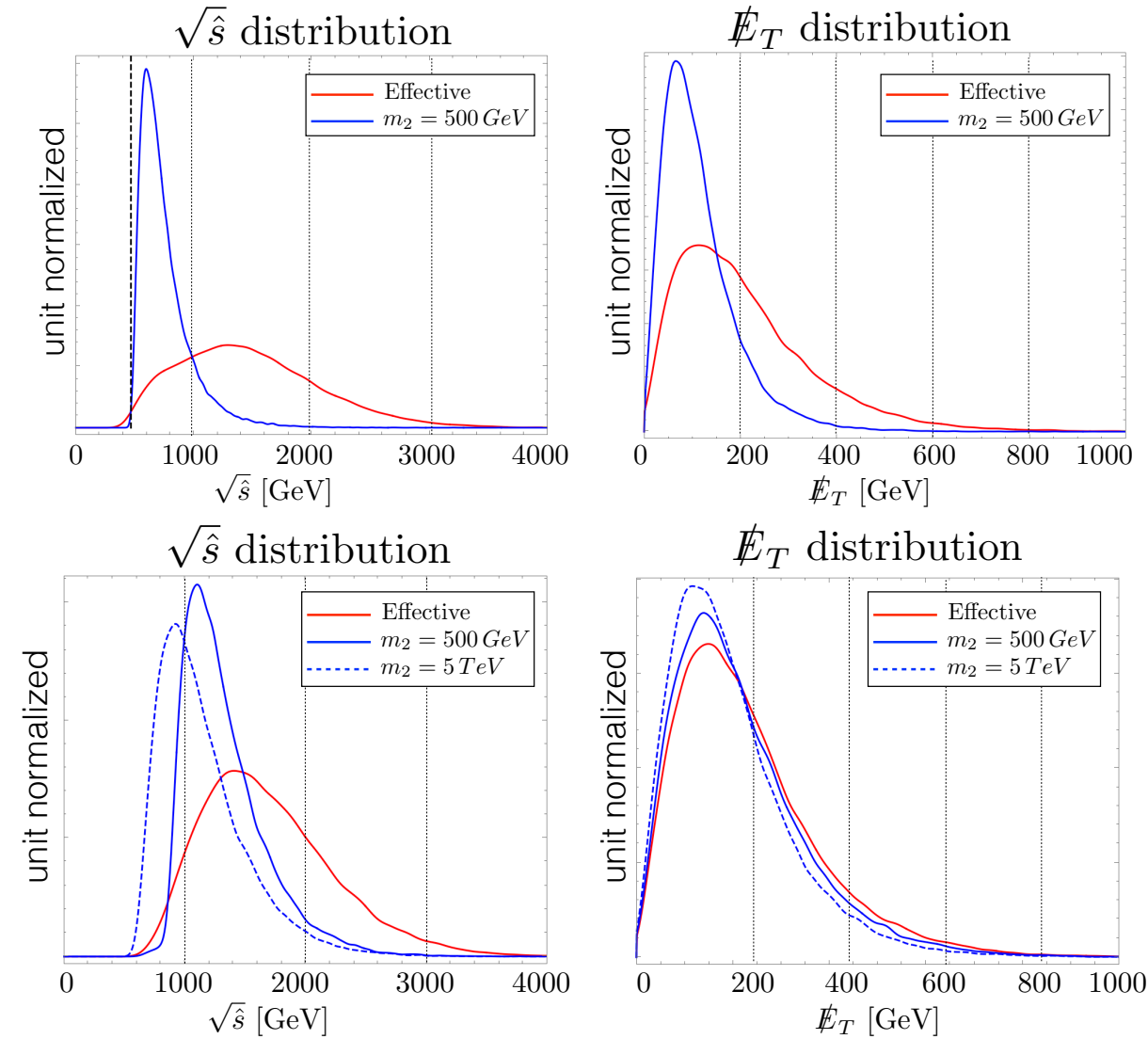


FIG. 2: Parton level distributions of various variables in a  $(t\bar{t}\chi\bar{\chi})$  channel for a dark matter's mass  $m_\chi = 10 \text{ GeV}$  (above) and  $m_\chi = 100 \text{ GeV}$  (below) for LHC 8TeV. As we can see here, due to a higgs propagator, even when  $m_2 \rightarrow \infty$  case, a missing transverse energy  $\cancel{E}_T$  of a higgs portal model shall be different from an effective operator operator case.

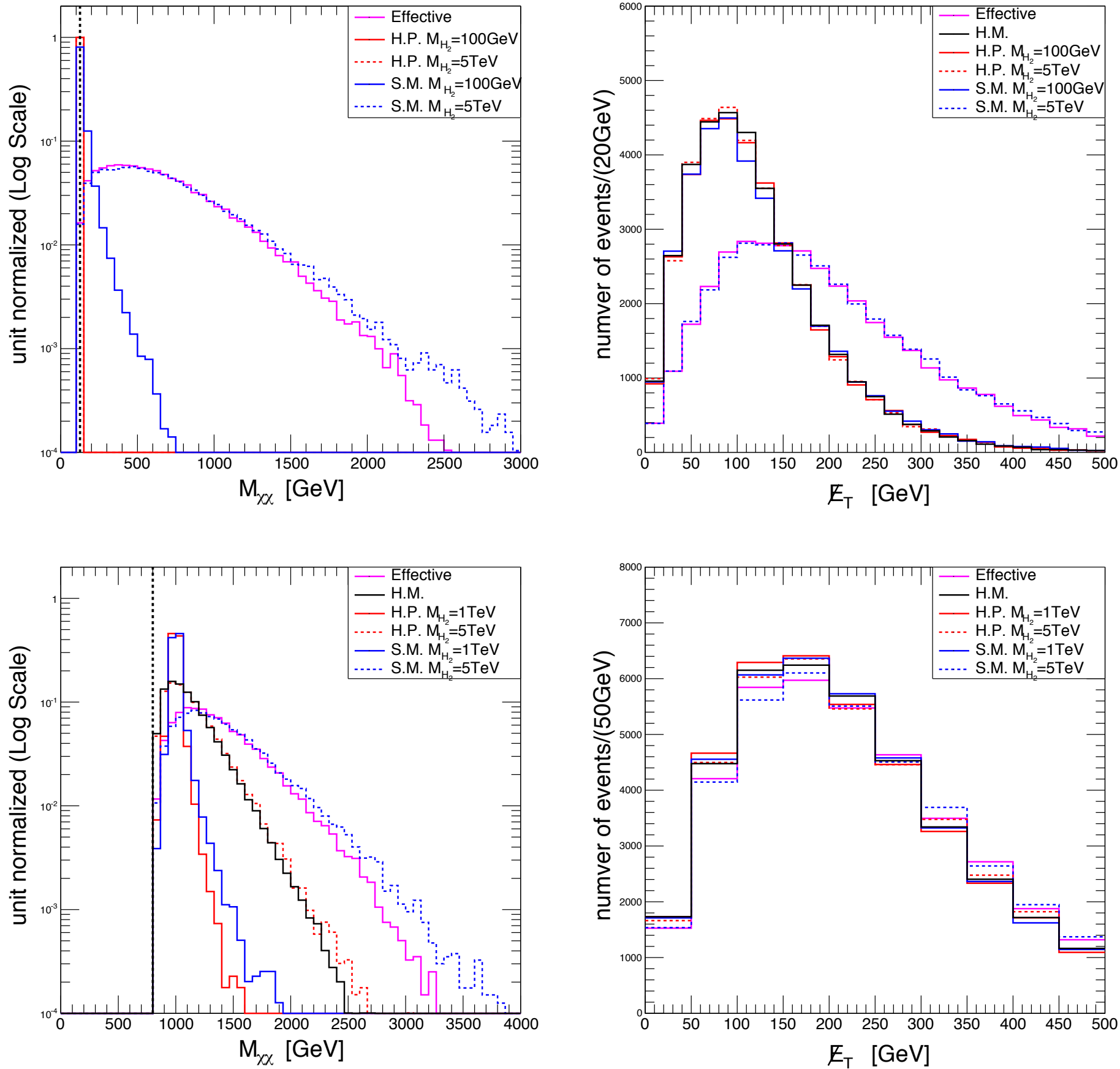


FIG. 4: With CMS 8TeV  $t\bar{t} + \cancel{E}_T$  search [6], we plot  $M_{\chi\chi}$  and the  $\cancel{E}_T$  in a reconstruction level. Upper panels are with  $M_\chi = 50$  GeV and lower panels are of  $M_\chi = 400$  GeV.

- EFT : Effective operator  $\mathcal{L}_{int} = \frac{m_q}{\Lambda_{dd}^3} \bar{q}q\bar{\chi}\chi$
- S.M.: Simple scalar mediator  $S$  of  

$$\mathcal{L}_{int} = \left( \frac{m_q}{v_H} \sin \alpha \right) S \bar{q}q - \lambda_s \cos \alpha S \bar{\chi}\chi$$
- H.M.: A case where a Higgs is a mediator  

$$\mathcal{L}_{int} = - \left( \frac{m_q}{v_H} \cos \alpha \right) H \bar{q}q - \lambda_s \sin \alpha H \bar{\chi}\chi$$
- H.P.: Higgs portal model as in eq. (2).

$$\text{H.P.} \xrightarrow[m_{H_2}^2 \gg \hat{s}]{} \text{H.M.},$$

$$\text{S.M.} \xrightarrow[m_S^2 \gg \hat{s}]{} \text{EFT},$$

$$\text{H.M.} \neq \text{EFT}.$$

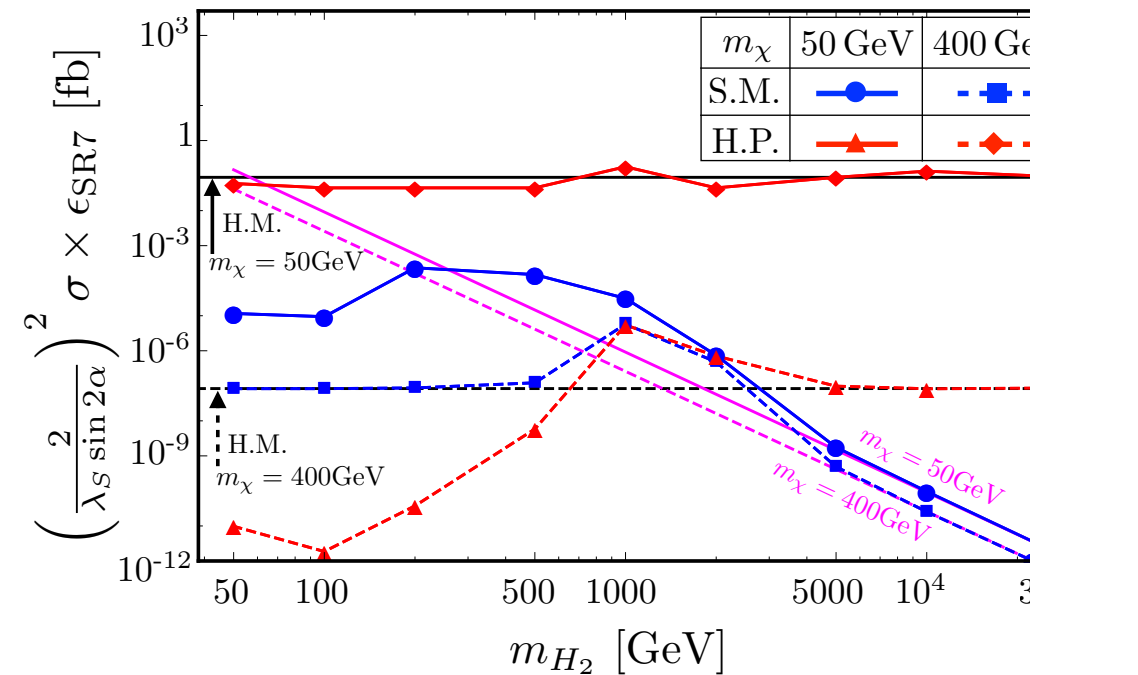


FIG. 2: Rescaled cross sections for the monojet+ $\cancel{E}_T$  in the signal region SR7 ( $\cancel{E}_T > 500$  GeV) at ATLAS [11]. Each line corresponds to the EFT approach (magenta), S.M. (blue), H.M. (black), and H.P. (red), respectively. The solid and dashed lines correspond to  $m_\chi = 50$  GeV and 400 GeV in each model, respectively.

- EFT : Effective operator  $\mathcal{L}_{int} = \frac{m_q}{\Lambda_{dd}^3} \bar{q}q \bar{\chi}\chi$
- S.M.: Simple scalar mediator  $S$  of  

$$\mathcal{L}_{int} = \left( \frac{m_q}{v_H} \sin \alpha \right) S \bar{q}q - \lambda_s \cos \alpha S \bar{\chi}\chi$$
- H.M.: A case where a Higgs is a mediator  

$$\mathcal{L}_{int} = - \left( \frac{m_q}{v_H} \cos \alpha \right) H \bar{q}q - \lambda_s \sin \alpha H \bar{\chi}\chi$$
- H.P.: Higgs portal model as in eq. (2).

$$\begin{aligned} \text{H.P.} &\xrightarrow[m^2_{H_2} \gg \hat{s}]{} \text{H.M.}, \\ \text{S.M.} &\xrightarrow[m^2_S \gg \hat{s}]{} \text{EFT}, \\ \text{H.M.} &\neq \text{EFT}. \end{aligned}$$

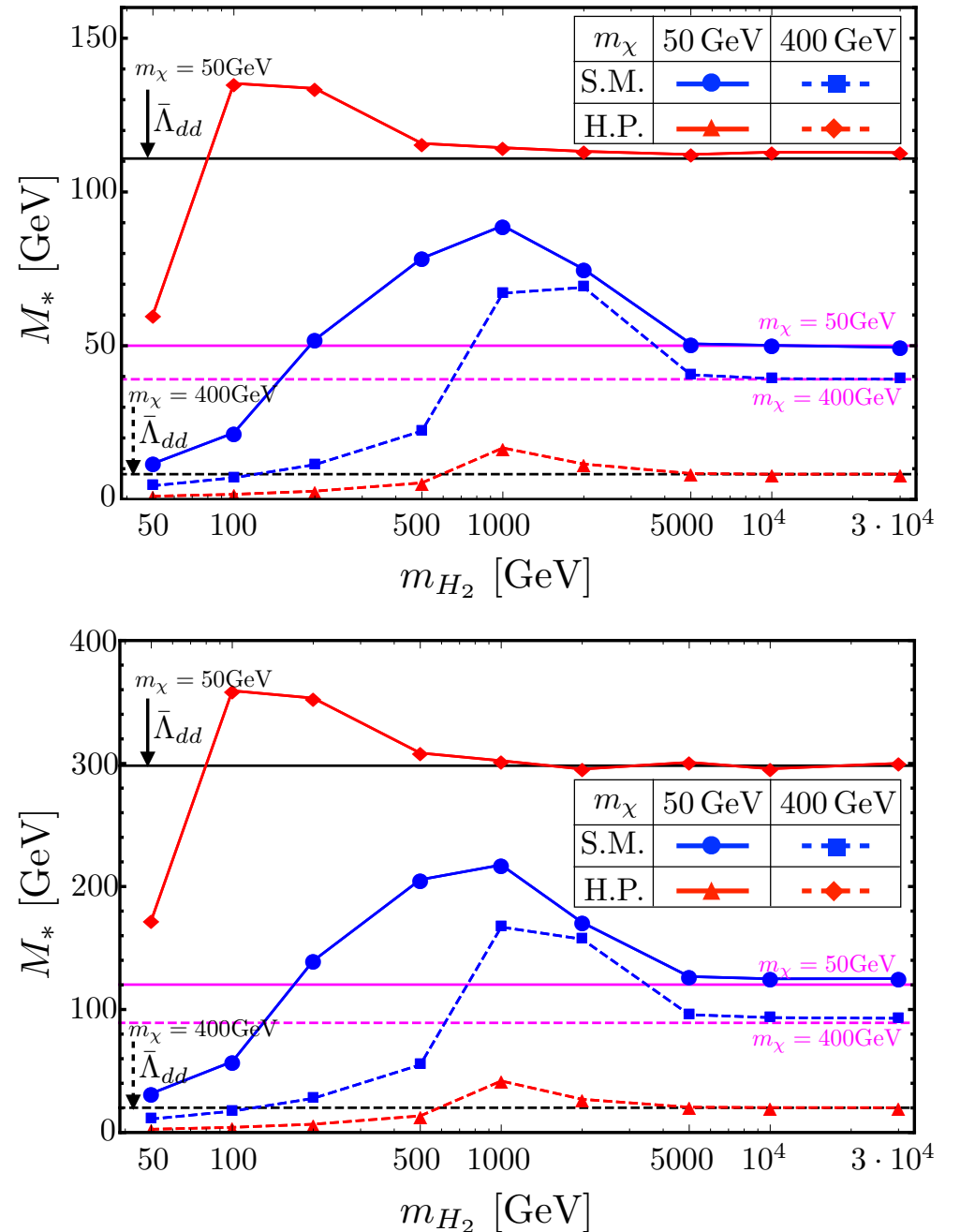


FIG. 3: The experimental bounds on  $M_*$  at 90% C.L. as a function of  $m_{H_2}$  ( $m_S$  in S.M. case) in the monojet+ $\cancel{E}_T$  search (upper) and  $t\bar{t}$ + $\cancel{E}_T$  search (lower). Each line corresponds to the EFT approach (magenta), S.M. (blue), H.M. (black), and H.P. (red), respectively. The bound of S.M., H.M., and H.P., are expressed in terms of the effective mass  $M_*$  through the Eq.(16)-(20). The solid and dashed lines correspond to  $m_\chi = 50$  GeV and 400 GeV in each model, respectively.

# A General Comment

**assume:**  $2m_\chi \ll m_{125} \ll m_2 \ll \sqrt{s}$

$$\begin{aligned}\sigma(\sqrt{s}) &= \int_0^1 d\tau \sum_{a,b} \frac{d\mathcal{L}_{ab}}{d\tau} \hat{\sigma}(\hat{s} \equiv \tau s) \\ &= \left[ \int_{4m_\chi^2/s}^{m_{125}^2/s} d\tau + \int_{m_{125}^2/s}^{m_2^2/s} d\tau + \int_{m_2^2/s}^1 d\tau \right] \sum_{a,b} \frac{d\mathcal{L}_{ab}}{d\tau} \hat{\sigma}(\hat{s} \equiv \tau s)\end{aligned}$$

**For each integration region for tau,  
we have to use different EFT**

**No single EFT applicable to the entire tau regions**

# Indirect Detection

$$\begin{aligned} \left| \frac{1}{\Lambda_{ann}^3} \right| &\simeq \frac{1}{\Lambda_{dd}^3} \left| \frac{m_{125}^2}{4m_\chi^2 - m_{125}^2 + im_{125}\Gamma_{125}} - \frac{m_{125}^2}{4m_\chi^2 - m_2^2 + im_2\Gamma_2} \right| \\ &\rightarrow \frac{1}{\Lambda_{dd}^3} \left| \frac{m_{125}^2}{4m_\chi^2 - m_{125}^2 + im_{125}\Gamma_{125}} \right| \neq \frac{1}{\Lambda_{dd}^3} \end{aligned}$$

- Again, no definite correlations between two scales in DD and ID
- Also one has to include other channels depending on the DM mass

# Pseudoscalar portal DM

(S. Baek, P. Ko, Jinmian Li, arXiv:1701.04131)

$$\frac{1}{\Lambda^2} \bar{f} f \bar{\chi} \gamma_5 \chi$$

- Highly suppressed for SI/SD x-section
- DM pair annihilation in the S-wave

Its simplest UV completion:  
(different from 2HDM portal)

$$\begin{aligned} \mathcal{L} = & \bar{\chi}(i\partial \cdot \gamma - m_\chi - ig_\chi a\gamma^5)\chi + \frac{1}{2}\partial_\mu a\partial^\mu a - \frac{1}{2}m_a^2 a^2 \\ & - (\mu_a a + \lambda_{Ha} a^2) \left( H^\dagger H - \frac{v_h^2}{2} \right) - \frac{\mu'_a}{3!} a^3 - \frac{\lambda_a}{4!} a^4 \\ & - \lambda_H \left( H^\dagger H - \frac{v_h^2}{2} \right)^2. \end{aligned} \quad (1)$$

see also Karim Ghorbani, arXiv:1408.4929 [hep-ph]

# Interaction Lagrangians

$$\begin{aligned} \mathcal{L}_{\text{int}} = & -ig_\chi(H_0 \sin \alpha + A \cos \alpha) \bar{\chi} \gamma^5 \chi - (H_0 \cos \alpha - A \sin \alpha) \\ & \times \left[ \sum_f \frac{m_f}{v_h} \bar{f} f - \frac{2m_W^2}{v_h} W_\mu^+ W^{-\mu} - \frac{m_Z^2}{v_h} Z_\mu Z^\mu \right] \end{aligned} \quad (7)$$

**For comparison, let us define 2 other cases**

$$\begin{aligned} \mathcal{L}_{\text{int}}^{\text{SS}} = & -g_\chi(H_1 \sin \alpha + H_2 \cos \alpha) \bar{\chi} \chi - (H_1 \cos \alpha - H_2 \sin \alpha) \\ & \times \left[ \sum_f \frac{m_f}{v_h} \bar{f} f - \frac{2m_W^2}{v_h} W_\mu^+ W^{-\mu} - \frac{m_Z^2}{v_h} Z_\mu Z^\mu \right] \end{aligned} \quad (\text{Higgs portal}) \quad (12)$$

$$\begin{aligned} \mathcal{L}_{\text{int}}^{\text{AA}} = & -ig_\chi(a \sin \alpha + A \cos \alpha) \bar{\chi} \gamma^5 \chi \\ & - i(a \cos \alpha - A \sin \alpha) \sum_f \frac{m_f}{v_h} \bar{f} \gamma^5 f \end{aligned} \quad (\text{2HDM+a portal}) \quad (13)$$

# DM phenomenology

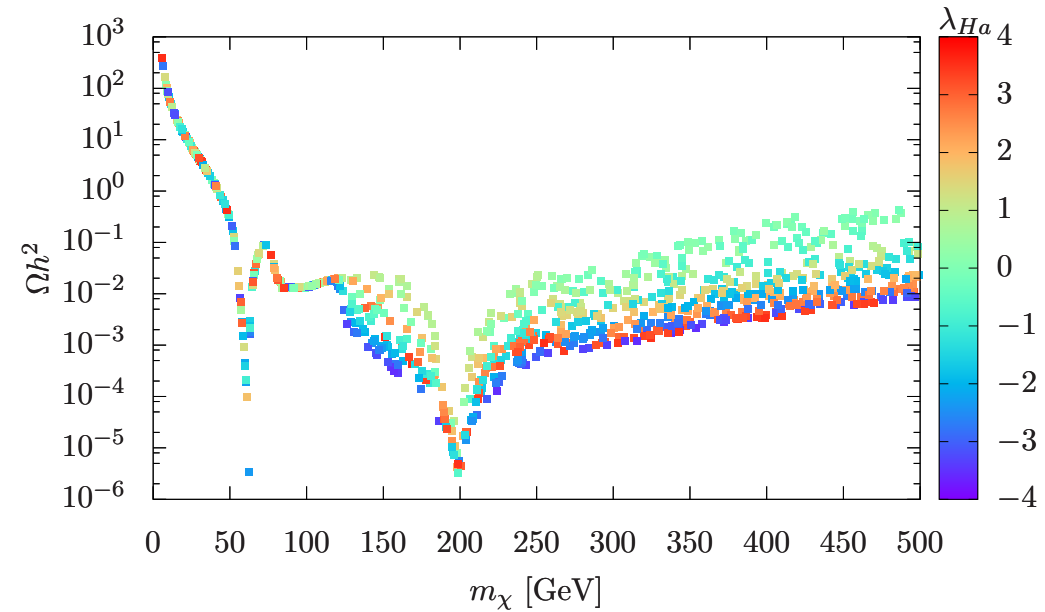


FIG. 1. Relic density with varying DM mass, for  $m_A = 400$  GeV,  $g_\chi = 1$  and  $\alpha = 0.3$ . Color code indicates the value of  $\lambda_{H^a}$ .

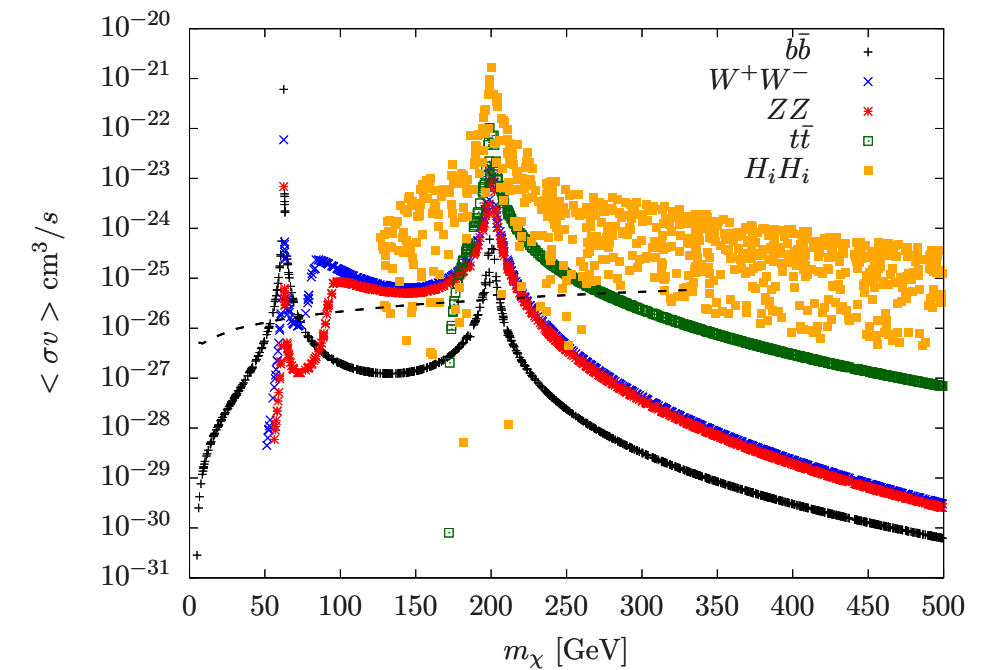


FIG. 2. The cross sections for different DM annihilation (at rest) channels. The dashed black curve correspond to the 95% CL exclusion limit on  $b\bar{b}$  channel obtained from Milky Way Dwarf Spheroidal Galaxies with Six Years of Fermi-LAT Data [55].

# Collider Searches

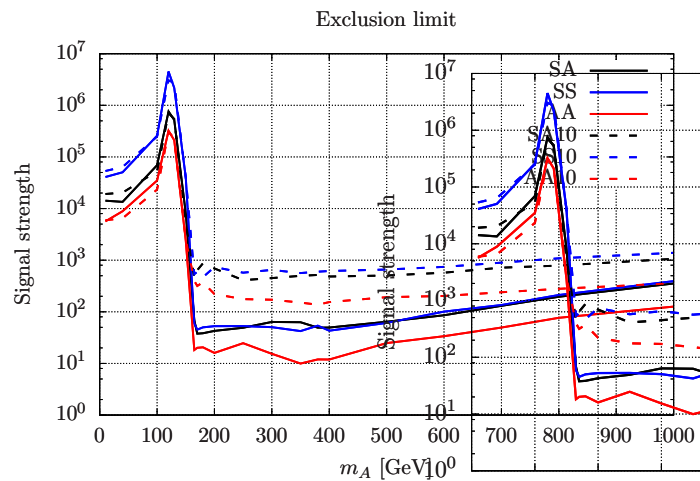


FIG. 5. The 95% CL exclusion limits from the ATLAS mono-jet search at 13 TeV with integrated luminosity of  $3.2 \text{ fb}^{-1}$ . The dashed curves correspond to models with ten times larger total width of  $A$  than  $\Gamma_{\min}$  due to the opening of new decay channels.

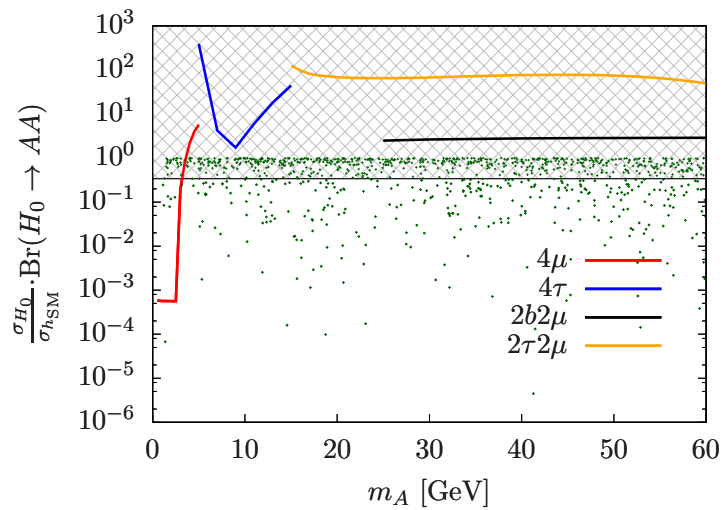


FIG. 7. Bounds correspond to the LHC searches for light boson pair from the SM Higgs decay. The shaded region is excluded by the Higgs precision measurement. Our models are shown by dark green points.

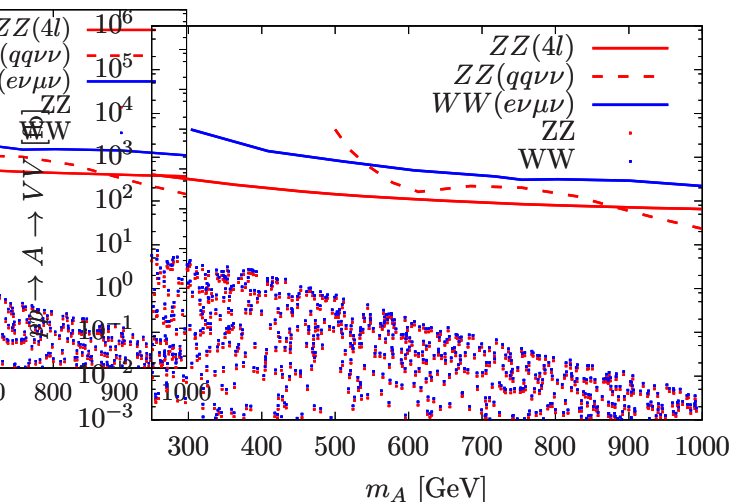


FIG. 6. Bounds correspond to the LHC searches for two vector boson resonance. The production cross sections of  $ZZ$  ( $WW$ ) at 13 TeV in our model are shown by red (blue) points.

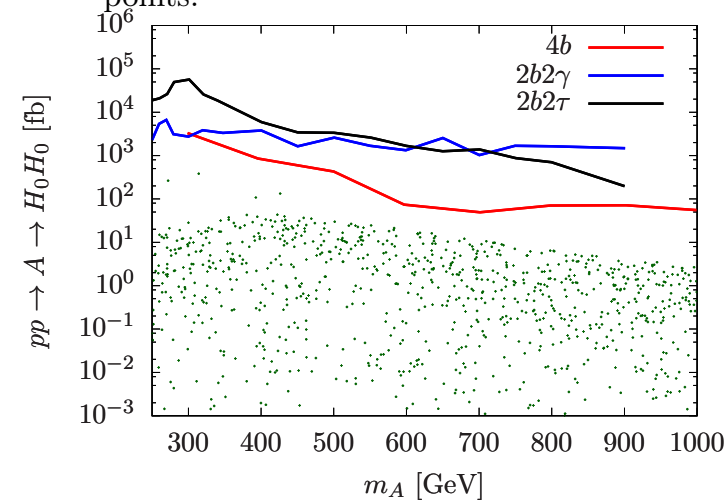


FIG. 8. Bounds correspond to the LHC di-Higgs searches in different final states. The production cross section of our models at 13 TeV are shown by dark green points.

# Conclusion

- Renormalizable and unitary model (with some caveat) is important for DM phenomenology (**EFT can fail completely**)
- Imposing the full SM gauge symmetry is crucial for collider searches for DM
- Usually two propagators necessary for UV completion of the effective operators >> **Important interference effects to be included in the data analysis**

# Conclusion

- Renormalizable and unitary model (with some caveat) is important for DM phenomenology (**EFT can fail completely**)
- Hidden sector DM with Dark Gauge Sym is well motivated, can guarantee DM stability/longevity, solves some puzzles in CDM paradigm, open a new window in DM models including DM-DR interaction
- Especially a wider region of DM mass is allowed due to new open channels

- DM Dynamics dictated by local gauge symmetry
- Non Standard Higgs decays into a pair of DM, light dark Higgs bosons, or dark gauge bosons, etc.
- Additional singlet-like scalar “S” (Dark Higgs) : generic, can play important roles in DM phenomenology, improves EW vac stability, helps Higgs inflation with larger tensor/scalar ratio (also strong 1st order ph tr. in the dark sector, GW, etc. ?) >> Should be actively searched for
- Searches @ LHC & other future colliders